NTNU
Norwegian University of
Science and Technology

SIMULATION AND EXPERIMENT RESEARCH ABOUT TWO-PHASE R744 EJECTOR SYSTEM

Jinrui Zhang

Sustainable Energy
Submission date: January 2016
Supervisor: Trygve Magne Eikevik, EPT
Co-supervisor: Jingyi Wu, School of Mechanical Engineering

Norwegian University of Science and Technology
Department of Energy and Process Engineering

NTNU

Norwegian University
of Science and Technology

Department of Energy
and Process Engineering

EPT-M-2014-118

MASTER THESIS

for

Student Jinrui Zhang

Spring 2015

Theoretical and experimental analysis of different two-phase R744 ejector cycles

Teoretiske og eksperimentelle analyser av to forskjellige tofase R744 ejektorsystemer

Background and objective

Much of the recent work on two-phase ejectors has been focused on transcritical CO_2 systems because of the high throttling loss and high potential for improvement associated with the throttling of transcritical CO_2 in the expansion valve cycle.

Several modifications to the standard two-phase ejector cycle of Gay (1931) have been proposed in the recent years. Two of these cycles, proposed by Burk et al. (2006) and Oshitani et al. (2005) do not require a liquid–vapor separator and they allow for evaporation at two different temperatures.

Therefore, the objective of the thesis is to present a comparison of three different two-phase ejector refrigeration cycles as well as a comparison to an expansion valve refrigeration cycle with two evaporation temperatures. An analytical comparison of the theoretical COPs of the ejector cycles shall be presented. Based on results of numerical simulations, appropriate modifications of the existing ejector test facility shall be carried out. The student will make the design of the modifications. Finally a set of experiments shall be planned and performed for different options of the ejector cycle (with vs. without vapor–liquid separator, single vs. dual evaporator, diffuser outlet split vs. condenser outlet split).

The following tasks are to be considered:

1. Literature review on R744 ejector technology
2. Development of 0D mathematical models for the R744 refrigeration cycles considered (standard transcritical, Gay cycle, Burk cycle, Oshitani cycle)
3. Implementation of individual ejector characteristics into the refrigeration cycle models
4. Carrying out a number of numerical simulations aimed at component sizing/dimensioning in the considered cycles
5. Modification/set up of the test facility in Room 3
6. Test campaign
7. Data processing and comparison analysis
8. Preparation of a scientific paper from the main results of the Master Thesis
9. Making suggestion for further work

-- ” --

Within 14 days of receiving the written text on the master thesis, the candidate shall submit a research plan for his project to the department.

When the thesis is evaluated, emphasis is put on processing of the results, and that they are presented in tabular and/or graphic form in a clear manner, and that they are analyzed carefully.

The thesis should be formulated as a research report with summary both in English and Norwegian, conclusion, literature references, table of contents etc. During the preparation of the text, the candidate should make an effort to produce a well-structured and easily readable report. In order to ease the evaluation of the thesis, it is important that the cross-references are correct. In the making of the report, strong emphasis should be placed on both a thorough discussion of the results and an orderly presentation.

The candidate is requested to initiate and keep close contact with his/her academic supervisor(s) throughout the working period. The candidate must follow the rules and regulations of NTNU as well as passive directions given by the Department of Energy and Process Engineering.

Risk assessment of the candidate's work shall be carried out according to the department's procedures. The risk assessment must be documented and included as part of the final report. Events related to the candidate's work adversely affecting the health, safety or security, must be documented and included as part of the final report. If the documentation on risk assessment represents a large number of pages, the full version is to be submitted electronically to the supervisor and an excerpt is included in the report.

Pursuant to "Regulations concerning the supplementary provisions to the technology study program/Master of Science" at NTNU §20, the Department reserves the permission to utilize all the results and data for teaching and research purposes as well as in future publications.

The final report is to be submitted digitally in DAIM. An executive summary of the thesis including title, student's name, supervisor's name, year, department name, and NTNU's logo and name, shall be submitted to the department as a separate pdf file. Based on an agreement with the supervisor, the final report and other material and documents must be given to the supervisor in digital format. All relevant data collected and produced during the project shall be delivered to the supervisor on a Memory stick at the end of the project.

☒ Work to be done in lab (Water power lab, Fluids engineering lab, Thermal engineering lab)
☐ Field work

Department of Energy and Process Engineering, March 3rd 2015

Prof. Olav Bolland
Department Head

Prof Trygve M. Eikevik
Academic Supervisor
e-mail: Trygve.m.eikevik@ntnu.no

Research Advisor(s):
Armin Hafner, SINTEF Energy Research
Krzysztof Banasiak, SINTEF Energy Research

e-mails
Armin.hafner@sintef.no
Krzysztof.Banasiak@sintef.no

SIMULATION AND EXPERIMENT RESEARCH ABOUT TWO-PHASE R744 EJECTOR SYSTEM

ABSTRACT

In this paper, the ejector theory and description of cycles are introduced at first. The following are experimental methods and the test facility modification. There are two test facilities involved in this thesis work. The first one is to give the overall view of the ejector performance. And the other one is to compare two systems performance using this ejector. Some simulation works present at last.

Experimental analyses of two experiments are presented. First one is overall view of ejector performance, it shows where the high efficiencies lies on the working conditions. The results can guide the test points choosing on the second experiment. Second one is comparison of two systems, which are Burk cycle (DOS) and Oshitina cycle (COS). The comparisons are about the two systems' COP and exergy increase in the evaporator side. Then the uncertainty analysis is introduced to complete the experimental analysis.

At last the computational simulation on the ejector and cycles are done. The ejector model is developed based on Kornhauser ejector model. The assumptions and the applied equations in the thermodynamic model are described below. The comparisons of the cycle model results and experimental results are also presented below. At last an expansion valve cycle is built to present how the ejector can help improving the system performance. Some limitation of the model are shown.

KEY WORDS：ejector，ejector cycles，COP，R744

Content

List of figures

List of tables

1. Introduction

With the destruction of the ozone layer, greenhouse effect and other environmental problems Increasing, the researches on environmentally friendly natural refrigerant CO_2 that as an alternative to working fluid has been increased. Much of the recent work on CO_2 systems has focused on transcritical CO_2 systems using two-phase ejectors. Because the two-phase ejectors can be used to reduce the inherent throttling losses of the expansion valve and transcritical CO_2 systems have high throttling losses.

When ejectors are used in refrigeration cycles at first, the ejectors mostly are used in two different refrigeration systems. One is a cycle introduced by Leblanc (1910) [1]. This cycle has a vapor jet ejector and can use waste heat energy sources in order to provide refrigeration. And this cycle can be more economical than the normal vapor compression refrigeration cycle. The other one is introduced by Gay (1931) [2]. Gay got a patent for using the two-phase ejector to reduce throttling losses. In the late 1980s, many researches focus on transcritical R744 (CO_2) cycles again, and then ejectors have been considered to improve the performance of the cycles. For now, a lot of studies of the R744 two-phase ejector have been published (see 2.), so it is a very promising way to improve the transcritical systems' efficiency.

On this thesis paper, we focus on three two-phase R744 ejector cycles. First one is the standard two-phase ejector cycle of Gay (1931). It is called as Gay cycle below. And two modifications of the standard two-phase Gay cycle will be discussed on the report. Second cycle is proposed by Burk et al. (2006) [20] and third cycle is proposed by Oshitani et al. (2005) [19]. These two cycles do not require a liquid-vapor separator and they allow for evaporation at two different temperatures. The comparison of the second and third two-phase ejector refrigeration cycles with two evaporation temperatures is presented. The comparison uses experimental methods and computational methods. And an analytical comparison of the theoretical COPs of the ejector cycle is presented.

This report begins with the development of the ejectors, which is a literature review of the published studies about the R744 two-phase ejector. The theory of ejector and the cycles the paper focused on is then given. Followed the theory part are the methodology we have used for our analysis, and how the modification we have done. Results, discussion, and conclusions are then presented.

2. Development of ejector

2.1 Historical back ground and the design of ejector

Ejectors are amazing mechanical devices. Eckhard (2011) introduces that a typical ejector consists of a motive nozzle, a suction nozzle or receiving chamber, a mixing section and a diffuser [4]. The motive stream with high pressure will exchange its internal energy in the motive nozzle. The motive stream expands and converts the internal energy into kinetic energy. In the suction nozzle, this converted motive stream with high speed can entrain a low pressure stream, which is suction stream. These two streams exchange momentum, kinetic and internal energies in the mixing section. With this mixing process, these two streams converge in one stream, which is equilibrium in pressure and speed. In order to reach a higher pressure than the inlet pressure of suction nozzle, this uniform flow changes its kinetic energy to internal energy in the diffuser [4]. With the understanding of the principle of ejector working process, many systems equipped with ejectors have been studied in simulation methods and experimental methods for many years. Maurice Leblanc established the first water vapor ejector refrigeration system in France at 1910, and the energy resource is heat [4]. In 1931, Gay improved the ejector model and it is a patent of Gay now. The research of ejector were on the common working fluids at first. Then the ejectors with two phase refrigerants were the topic of research in nineteen fifties. First, the energy resource of ejector was low-grade energy, which usually was solar energy or waste heat. The ejector cycle was using this kind of energy to operate. Then, with the time flied by, ejectors were also used in refrigeration cycles, which utilized expansion valve before (Kornhauser, 1990) [17]. Two-phase ejector can suck and increase the pressure of suction flow by replacing the expansion valve, which can be used for expansion of the refrigerant. It is possible to increase the COP of the system with the compression work reduced with a low pressure ratios. Kemper et al. (1966) [21] introduced an ejector cycle which was a common vapor compressor system utilizing the ejctor. Newton (1972a, 1972b) [22] got two patents of ejector research in the control part of the whole ejector cycle. Harrell and Konrhuaser found that in the normal refrigeration cycles, because the expansion losses are not that big, the two phase ejectors may not have advantage compare to the single phase ejectors [4]. But when the two-phase ejectors use on the transcritical R744 cycle, it would be different. Because the throttling part in a transcritical R744 cycle has relatively large irreversibility and R744's environmentally friendly characteristics, researches focus on transcritical R744 cycle equipped with ejector have growed recently.

As mentioned before, a typical ejector has four main part: a motive nozzle, a suction nozzle, a mixing section and a diffuser. Stefan Elbel (2011) [3] provides a literature review about the technology of ejector. He analyses some experimental results, and the experiment is completed in a transcritical R744 two-phase ejector cycle. In the ejector, a converging-diverging nozzle was designed as motive nozzle. And based on the model of Henry and Fauske (1971) the design of the motive nozzle is done [7]. Since there are significant speed difference that can cause large mixing losses between the two mixing flow. It is better use a variable size suction nozzle that can optimize the system performance. The size of suction nozzle and the mixing chamber are calculated by using a model. Also the diffuser outlet are using different angles. In these way the ejector can be test in different dimensions in order to optimize the ejector performance. And the performance of a transcritical R744 ejector cycle is compared to the performance of a normal expansion valve cycle. Form comparison of two cycles, it shows that the ejector can improved the performance of the system [3].

2.2 The use of ejectors

2.2.1 Ejector for utilization of low-grade energy

Fig. 1 shows the layout of a vapor jet ejector cycle which can harness a low-grade energy, and the corresponding pressure-specific enthalpy diagram involved. This cycle is for transcritical R744.

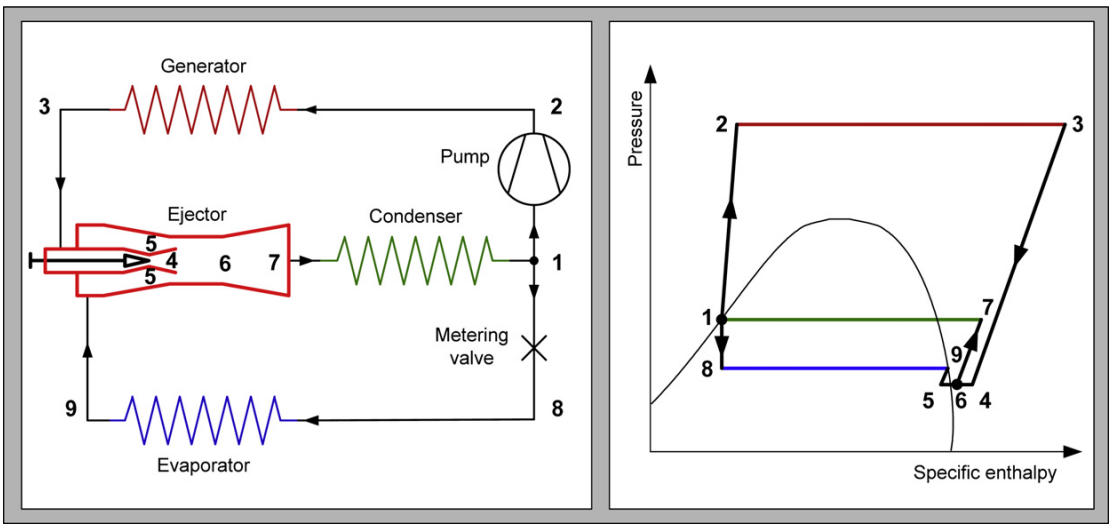

Figure 1 Transcritical R744 vapor het refrigeration cycle (Elbel, 2011)

The main advantage of this cycle is that it can utilize low grade energy as the energy resource to drive the refrigeration system, and the waste heat is commonly used to energize the generator.[24] This cycle is better than absorption system in that it does not need the mixture of working fluid. But both of these system can only achieve low COPs and require oversized condensers (Elbel, 2011) [1].

2.2.2 Ejector for recovery of expansion work

This type of ejector is what this paper mainly focuses on. A two phase ejector can improve the COP of a system by replacing an expansion valve to reduce the throttling losses. The setup of the cycle and the corresponding pressure-specific enthalpy diagram are shown in Fig. 2 below.

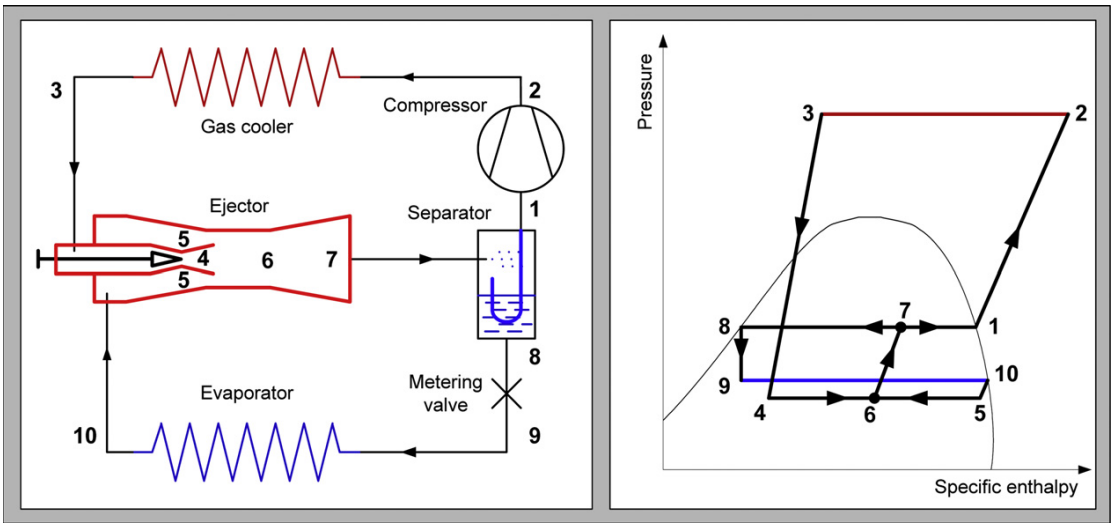

Figure 2 Transcritical R744 refrigeration cycle with a two-phase ejector (Elbel, 2011)

There are two main advantages of Gay's refrigeration cycle [1]. First, it can increase the cooling capacity due to the ejector can reduce the throttling loss than the normal expansion valve, which can cause larger cooling capacity in the evaporator. Second, the COP increases due to the compressor work reduces. A lot of investigations are focus on how much a two-phase ejector can improve a R744 transcritical system instead of an expansion valve. Ozaki et al. (2004) [5] present a research that shows the ejector system can improve 20% in COP over a normal expansion valve systems. Li and Groll (2005) [6] presents some simulation researches about R744 ejector in refrigeration systems. The result shows the ejector can improve the performance up to 16%. Elbel and Hrnjak (2004a) [8] show that the system can reach the best

performance by using ejector and internal heat exchanger, they can reduce the throttling losses of system.

2.2.3 Less commonly encountered ejector cycles

This part shows the ejector cycles that are not frequently used in the air-conditioning and refrigeration systems.

A new ejector cycle was provided by Bergander (2005) [9]. In this cycle, the use of the ejector is different from the normal ejector. It can increase the compressor discharge pressure. The setup of this ejector system and the corresponding pressure- specific enthalpy diagram are shown in Fig. 3. In the cycle there are a liquid pump and an ejector. They work together like another compressor. Because the isentropic pump work is far less than that of a compressor for the same pressure, COP can improve. However, these improvements are depend on the ejector efficiencies. And this cycle don't need lubrication R744 is a potential working fluid for this setup (Elbel, 2011) [1].

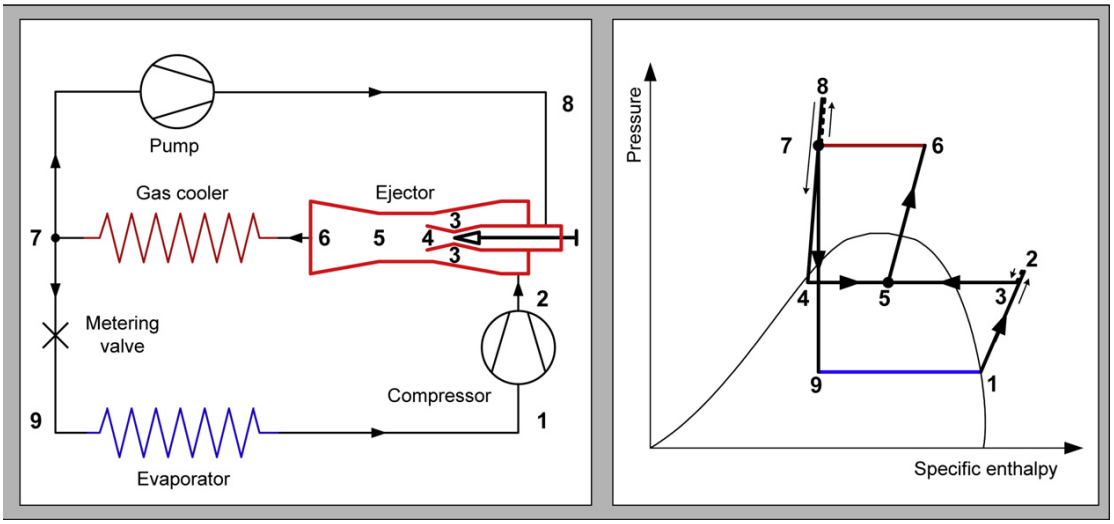

Figure 3 Ejector cycle using expansion work to drive liquid recirculation through the evaporator (Lorentzen, 1983)

2.3 New progresses on R744 ejector systems

2.3.1 Numerical analysis

Liu and Groll (2013) [10] presented a method to show the internal-ejector part efficiencies. Measured and simulation data were used to calculate the isentropic efficiencies of the motive nozzle, the suction nozzles, and the mixing section. The concept of the mixing efficiency is based on a momentum conservation equation that included the effects of pressure lift over the mixer. However, the definition of the mixing efficiency may be limited for two reasons, Banasiak et al. (2014) [11]. Firstly, it only can use on constant-diameter channels. Secondly, it neglect the irreversibility generated in the fluid core. And the effects of the individual efficiencies on the overall ejector efficiency were not examined.

Smolka et al. (2013) [12] presents another simulation model of ejector, which was established to simulate the transcritical compressible flow of a real fluid occurring in an ejector before. Their main aim was to build a numerical model for the two-phase R744 flow occurring in an ejector. The methodology used CFD that can show the property of two-phase flow especially for the case CO2 ejector [26].

Lawrence and Elbel (2013) [3] compared the standard two-phase ejector refrigeration cycle to two alternate two-phase ejector cycles without liquid vapor separator. These two cycle are COS (condenser outlet split) ejector cycle and DOS (diffuser outlet split) ejector cycle. Their layouts are shown in the next chapter (they are the main cycles discussed in this paper). An analytical comparison of the different cycles' theoretical COP shows that they have the same theoretical COP. Although they have the same theoretical COP, the standard cycle has lower availability destruction and higher Second Law efficiency than others [3]. The COS and DOS ejector cycles have advantages that they can offer more than one evaporation temperature and the liquid vapor separator is not needed in the cycles. The standard two-phase ejector cycle with a liquid vapor separator has the advantage that it can improve the evaporator performance because the quality of fluid is very low in the evaporator. When comparing the COS and DOS ejector cycles to each other, the COS ejector cycle has important advantages in considering oil return and operation at off-design conditions for the ejector [3]. The COS of ejector cycle COP can theoretically never fall below that of a normal expansion valve cycle and the cycle has important advantages in oil return. Due to these advantages, the focus of this paper would be on these alternate ejector cycles.

Banasiak et al. (2014) investigated the energy performance of two-phase R744 ejectors which can reduce the throttling losses [11]. They focused on the numerical analysis of different three levels in local- and global-flow irreversibility of the mixer mass flow. And these three levels represent three dissimilar flow patterns [29]. A previously developed CFD tool by Smolka et al. (2013) was used in the analysis [12]. And the numerical sensitivity analysis on the ejector performance shows that the method is useful. A complex mechanism of the physical dependencies between the ejector geometry and the ejector performance has been shown. It had conclusion that the future focus on ejector optimization procedures should concentrate on the entire ejector geometry.

Dokandari et al. (2014) was using the R744 and R717 as refrigerant to see the thermodynamical influence the performance of cascade cycle [13]. The theoretical analysis shows that the maximum COP and the maximum second law efficiency are on average 7% and 5% higher than the normal cycle and the exergy destruction ratios about 8 % lower than the conventional cycle. So we can say this ejector cascade cycle is a wonderful refrigeration cycle. The setup of this cycle with R744 and R717 and the corresponding pressure- specific enthalpy diagram are shown in Fig.4.

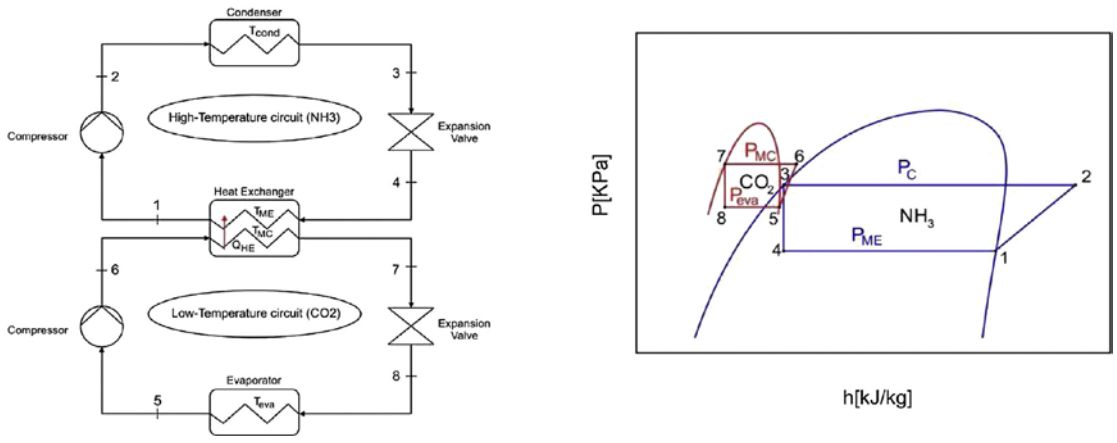

Figure 4 Ejector-expansion cascade cycle using R744 and R717 (Dokandari et al., 2014)

Meibo Xing et al. (2014) study on that two ejectors of a two-stage transcritical R744 heat pump cycle as expansion devices that can enhance the cycle COP [14]. The two ejectors were used to reduce as much throttling losses as they can, are located in low and high pressure stages. The performance of the system is evaluated in the mathematical model established before. And the comparison with the normal two-stage cycle is done. By further incorporating an internal

heat exchanger, the heating COP can be increased by 10.5–30.6% above that of the baseline cycle in the test conditions. The layout for such two-stage transcritical CO_2 system are shown in Fig 5.

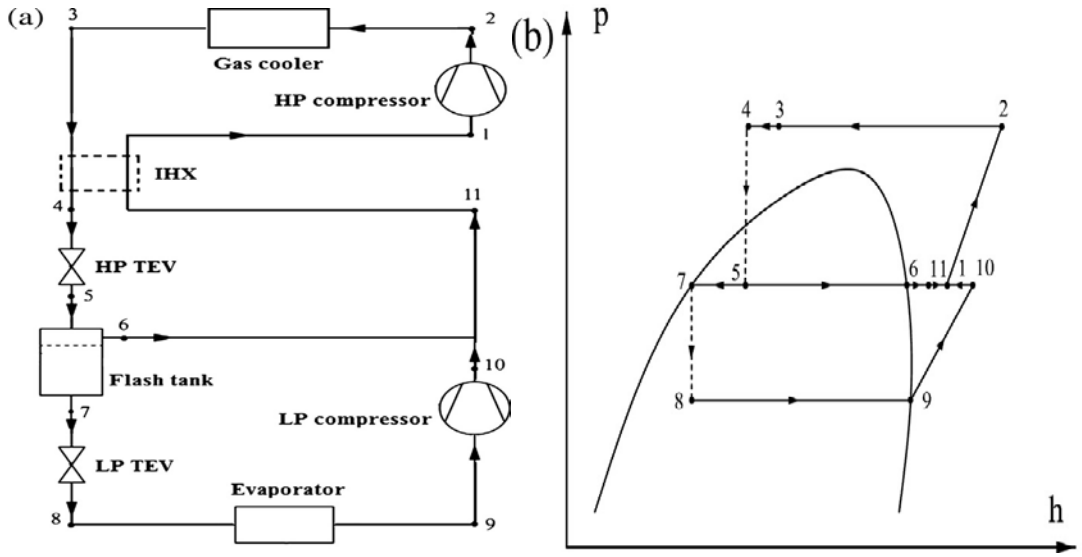

Figure 5 Two-stage transcritical R744 system and the corresponding pressure- specific enthalpy diagram (Meibo Xing et al., 2014)

Lucas et al. (2014) use CFD simulations to know of two-phase R744 ejectors' working conditions better and it can also help to design promising ejectors [15]. This numerical model is based on the homogeneous equilibrium approach. In their work, it is presented simulation analysis of an ejector in different operating conditions. And the comparison with experimental data is done to confirm the accuracy of the model. At the operating conditions without a suction flow, there are no mixing losses occuring and the friction losses became the main influence that influent the flow. So, this method can make accurate prediction of the friction losses by using simulation methods. The mixing losses if numerical results are comparing to the experimental data of an ejector which is operated with a suction mass flow. At the conditions without a suction flow, the pressure recovery is predicted within an error margin of 10%. At the conditions with a suction flow, the error margin increases to 20%. This differences show that the mixing losses are predicted less accurate.

Banasiak and Eikevik et al. (2014) numerically analyzed a sample about geometry of the R744 vapor ejector base on CFD [11]. The performance of ejector which is the efficiency of

ejector, was studied on numerical methods for three different boundary conditions. In all the cases of their study, it shows that the total irreversibility is less than 15% for the motive nozzle and suction nozzle, which is a relatively low percentage of it. But on the other hand, the losses were 49% and 63% for mixer and diffuser, which are high. Each source (turbulence, shock waves etc.) was simulated respectively on the contribution to the change of flow structure. An extraordinary simulation case that the motive flow rate and suction flow rate are well fitted is studied on experimental methods. The results shows there is a discrepancy of 23% of measured results and simulation results, resulting in over predicting the ejector efficiency of 15%.

2.3.2 Experimental analysis

Silvia Minetto et al. (2013) introduces the experimental research of a two phase ejector in a model R744 cycle [16]. Experiments shows that the ejector can really improve the cycle's COP. So this kind of R744 cycle also useful for normal heating and refrigeration use. However, problems related to the recovery of the lubricating oil from the low pressure side of the circuit has been discovered. So, appropriate system for oil recovery must be put in this kind of cycle.

Banasiak and Eikevik et al. (2014) presents an experimental analysis about a new test facility that equipped with a newly developed multiple ejector system [11]. The system, in parallel with a classical expansion valve, equips six different ejectors. The system shows increased flexibility compared to the standard R744-ejector refrigeration cycle. And this increased flexibility can ensure ejector operating over a wide range of operating conditions efficiently. The test facility can also give the entire efficiency maps for future commercial use. The efficiency maps will be used to design and choose the operational phase of R744 ejector refrigeration systems. Up to 30%, the efficiencies can be in certain operational conditions in the experimental results.

2.4 Summary of this chapter

In this chapter, it shows the development of ejector. At first, this chapter presents the historical background and design the ejector. Then the common use and uncommon use of

ejector are shown in the following including the ejector utilizing low grade energy, the ejector utilized for recovery expansion work and the less commonly used ejector. At last, some new progresses on R744 ejector systems are introduced, including numerical analysis and experimental analysis.

3. Ejector theory and cycle descriptions

3.1 The ejector theory

3.1.1 The R744 ejector working principle

Nowadays, with the destruction of the ozone layer, greenhouse effect and other environmental problems increasing, the researches on environmentally friendly natural refrigerant CO_2 that as an alternative to working fluid has been increased [28].

Carbon dioxide, or R744, has a low critical temperature which is 31.3 ^{o}C, and a high critical pressure which is 7.38 MPa. Due to these characteristics of R744, transcritical operation is more suitable for this working fluid. However one great drawback of this transcritical cycle is the large thermodynamic losses connected to the throttling of the working fluid. Many researchers try to improve the system's energy efficiency. And replacing the expansion valve with a two-phase ejector is one way to reduce the throttling losses [30].

A two-phase ejector is a device combined pump and expansion. Ejector consists of a motive nozzle, a suction nozzle or receiving chamber, a mixing section and a diffuser. It can utilize a high-pressure fluid from motive nozzle to entrain and increase the pressure of a low-pressure fluid from suction nozzle. A motive stream (high-pressure fluid) expands in the motive nozzle to a high velocity and low pressure. And this high velocity motive stream can be used to entrain that low-pressure fluid (suction stream). The two streams are mixed in mixing section, then enter diffuser, where they can be decelerated and compressed to a high pressure which is higher than the suction stream, and become a two-phase fluid to exit the ejector. The result is a pressure increase provided to the low-pressure vapor that is being pumped by the high-pressure liquid. In this way, the ejector promotes the circulation and provides pre-compressing to the refrigerant.

The ejector is a simple static device, but the performance prediction and analysis is a very complicated work due to several aspects regarding ejector flow. There are two key principles about the ejector: The Venturi-effect (occurring in the motive nozzle), and the momentum conservation between the two fluid streams in the mixing chamber (3). As seen in figure 1, the ejector's motive stream is accelerated through a converging-diverging nozzle (1), transforming a large amount of the energy in the motive stream into kinetic energy. As seen in figure 1, the motive stream exits the nozzle with a high velocity (and high kinetic energy content). In the

pre-mixing and mixing sections this motive flow with high velocity will mix with the fluid from suction nozzle (3), and they will exchange momentum. As these mixing flows get accelerated, a low pressure region can exist in the mixing chamber (3). Because of this low pressure region, the vapor from the suction accumulator gets continuously entrained into the ejector from suction nozzle (2). At the end of the mixing chamber, there is a diffuser converts some of the kinetic energy of the stream into pressure energy (4). The ejector thus works as a motive flow driven fluid pump which entrains and increases the static pressure of the secondary flow.

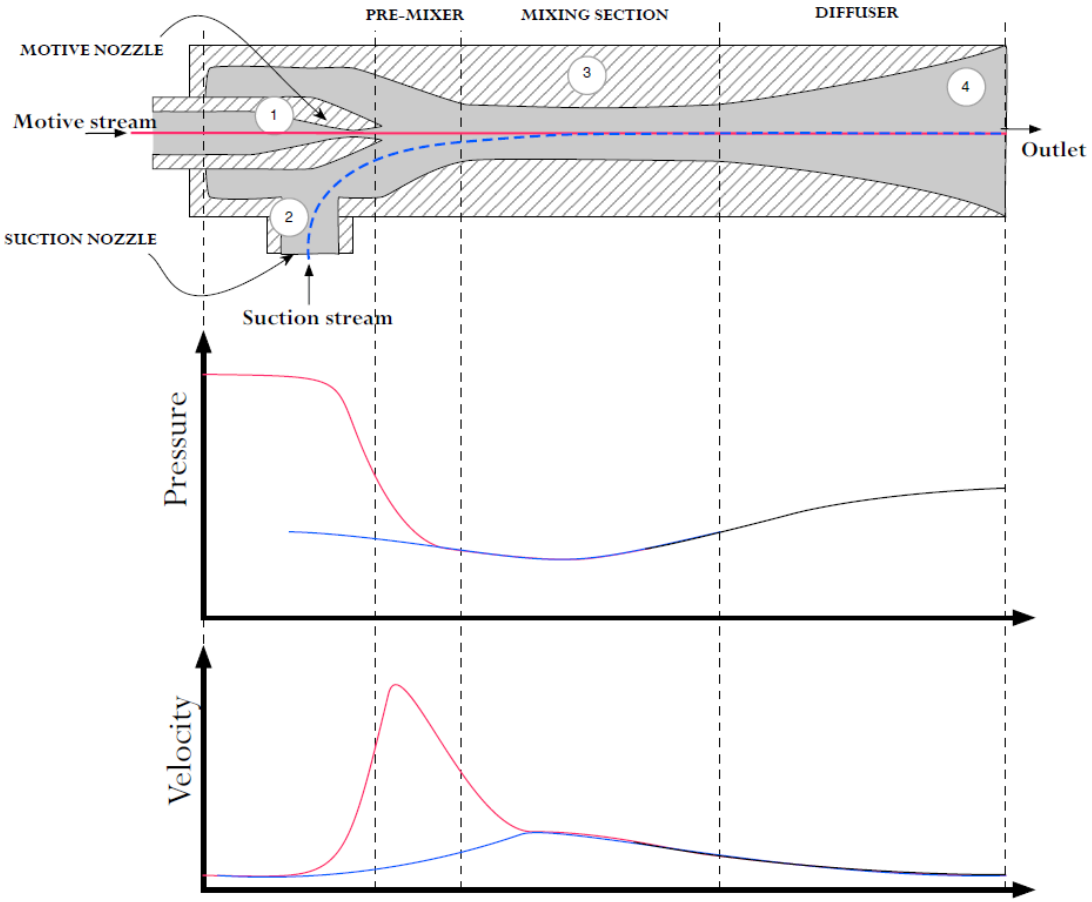

Figure 6 Principle of ejector along with pressure and velocity profiles

3.1.2 The ejector performance

Because of different fluid dynamical phenomena occurring inside the ejector such as shock waves, turbulence generation, friction etc., the ejector is working apart from an ideal process. So it is necessary to use the overall efficiency of the ejector to summarize the irreversibility generated by these different phenomena occurring under certain conditions.

In this two-phase ejector refrigeration test facility, there are different degrees of freedom for each boundary condition:

Table 1 Degrees of freedom for the two phase ejector

Motive nozzle	Pressure and temperature
Suction nozzle	Pressure, steam quality and temperature
Outlet	Pressure

It can be seen that there are two independent inlet conditions, so a clearly defined operating condition is depending on five variable parameters. Because of this, the work of ejector efficiency description, optimization and mapping will be a difficult and time consuming process.

In Elbel's doctoral thesis (2007), he presented an efficiency formulation of ejector based on the first law of thermodynamics. It can be seen in equation 3.1. It is the expansion work recovered to the maximum work recovery potential. Figure 2 can illustrate these motive stream and suction stream states.

$$\eta_{ejector} = \frac{\dot{W}_{rec}}{\dot{W}_{\max\ rec}} \tag{3.1}$$

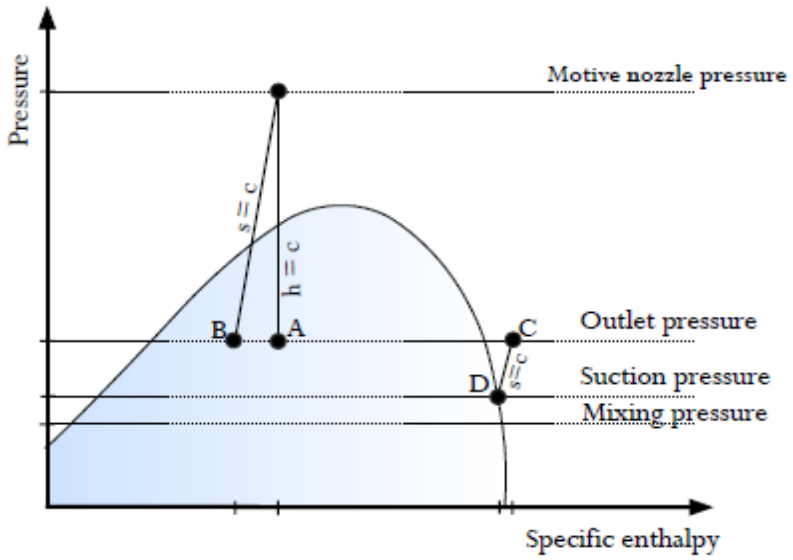

Figure 7 Pressure-enthalpy diagram along with imagined process lines used defining ejector efficiency Adapted and modified by Elbel (2007).

The maximum work recovery possibility is represented by the difference in enthalpy between state A and B. While the minimum work required compressing the suction flow is represented by states D and C.

So the maximum work recovery possibility can be expressed as:

$$\dot{W}_{\max\ rec} = \dot{m}_{MN} \int_{s_A}^{s_B} T_{diff.out}\, ds \tag{3.2}$$

As pressure A is equal pressure B, equation 3.2 can use equation 3.3, and because the last term in equation 3.3 is zero.

$$\mathrm{Tds} = \mathrm{dh} - \nu\mathrm{dp} \tag{3.3}$$

So

$$\dot{W}_{\max\ rec} = \dot{m}_{MN}(h_A - h_B) \tag{3.4}$$

Then the expansion work recovery can be expressed as:

$$\dot{W}_{rec} = \dot{m}_{SN} \int_{P_D}^{P_C} v(P) dP \tag{3.5}$$

This assumption of isentropic compression from state D to C will be the most conservative estimation. Use the equation 3.3, equation 3.5 can be rewritten as:

$$\dot{W}_{rec} = \dot{m}_{SN}(h_C - h_D) \tag{3.6}$$

Then the equation 3.1 can be:

$$\eta_{ejctor} = \phi \cdot \frac{h_C - h_D}{h_A - h_B} \tag{3.7}$$

ϕ is the mass entrainment ration that is defined as the ratio suction mass flow rate to the motive mass flow rate.

$$\phi = \frac{\dot{m}_{SN}}{\dot{m}_{MN}} \tag{3.8}$$

Therefore, the efficiency of the ejector can be estimated from the parameters obtained from external measurements of temperature and pressure with high certainty.

3.2 Description of the Gay cycle

Gay (1931) was the first person to propose the use of the two-phase ejector for work recovery application in a refrigeration system. So the basic transcritical R744 ejector cycle is depend on his idea. The cycle has become the standard cycle for transcritical R744 ejector cycle and been the focus for the majority of the ejector studies. This cycle uses a two-phase ejector as expansion mechanism and has a liquid-vapor separator. The refrigerant flow from the separator is separated to two flows. The vapor is compressed and cooled through the gas cooler, and then enter the motive nozzle of the ejector. The liquid is going to the evaporator to evaporate to vapor, and then enter the suction nozzle of the ejector. The motive stream entrains the suction stream, and then mixed in the mixing chamber. In this way, the ejector can improve the performance the cycle. Figure shows the layout of the Gay cycle and the corresponding P-h diagram.

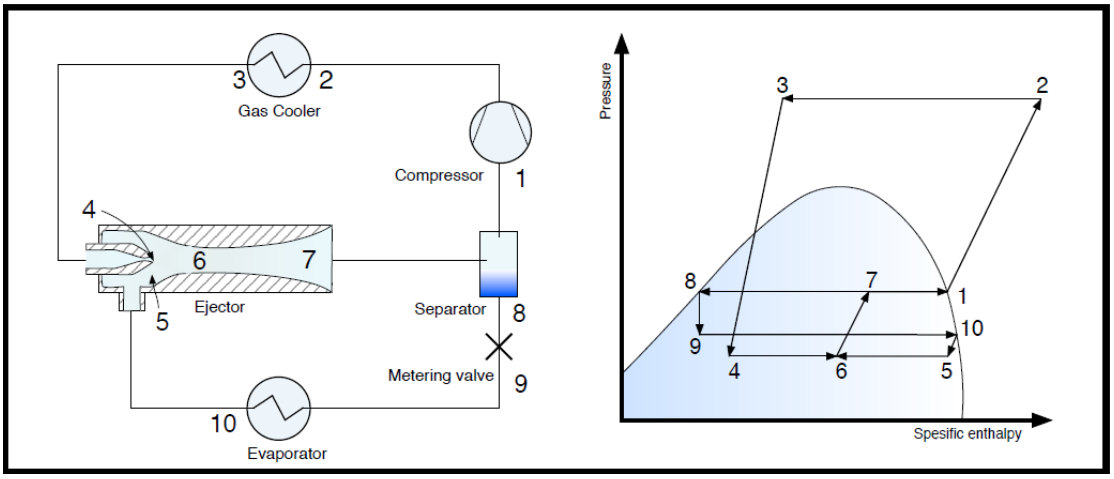

Figure 8 Basic transcritical R744 ejector cycle with corresponding pressure enthalpy diagram (Modified from Elbel, 2007)

3.3 Description of the Burk cycle

Burk et al. (2006) proposed a two-phase ejector cycle similar to Gay cycle. In Burk cycle, at the diffuser outlet of the ejector the flow split to two evaporators. One is high-temperature evaporator and the other is low-temperature evaporator. The flow through the low-temperature evaporator will be the suction flow entrained to the ejector (suction stream). The flow through the high-temperature evaporation will enter the compressor. This cycle does not need a liquid-vapor separator, and has two evaporators that allow two different evaporation temperatures. As

the characteristics this cycle has, it also is called as diffuser outlet split ejector cycle (DOS ejector cycle). Figure shows the layout of the Burk cycle and the corresponding P-h diagram.

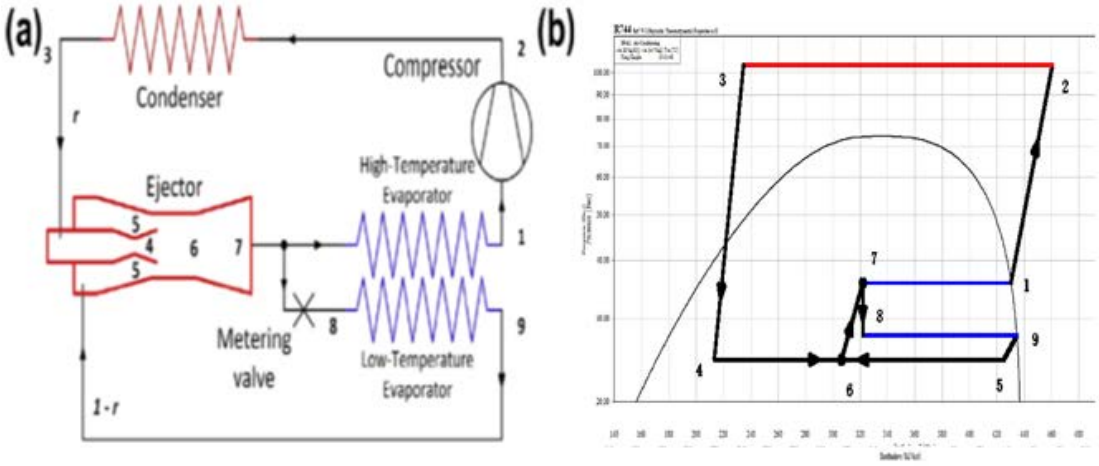

Figure 9 Burk cycle layout and corresponding pressure enthalpy diagram (Modified from Lawrence and Elbel, 2013)

3.4 Description of the Oshitani cycle

Oshitani et al. (2005) proposed another ejector cycle different from Gay cycle. In Oshitani cycle the flow out of ejector is sent directly into the compressor through a high-temperature evaporator. At the outlet of the condenser the flow split into two flows. One enters the ejector as motive steam. The other is sent directly to the low-temperature evaporator through an expansion valve. And this flow is entrained to ejector as suction stream. So this cycle does not have a liquid-vapor separator either. And it also has two evaporation temperatures too. Because of the pressure increase with the ejector, there will be a saturation temperature increase between the suction of the ejector and the diffuser of the ejector. This causes the different evaporation temperatures in the two evaporators. Due to the characteristics of the Oshitani cycle, it also is called as condenser outlet split ejector cycle (COS ejector cycle). Figure shows the layout of the Oshitani cycle and the corresponding P-h diagram.

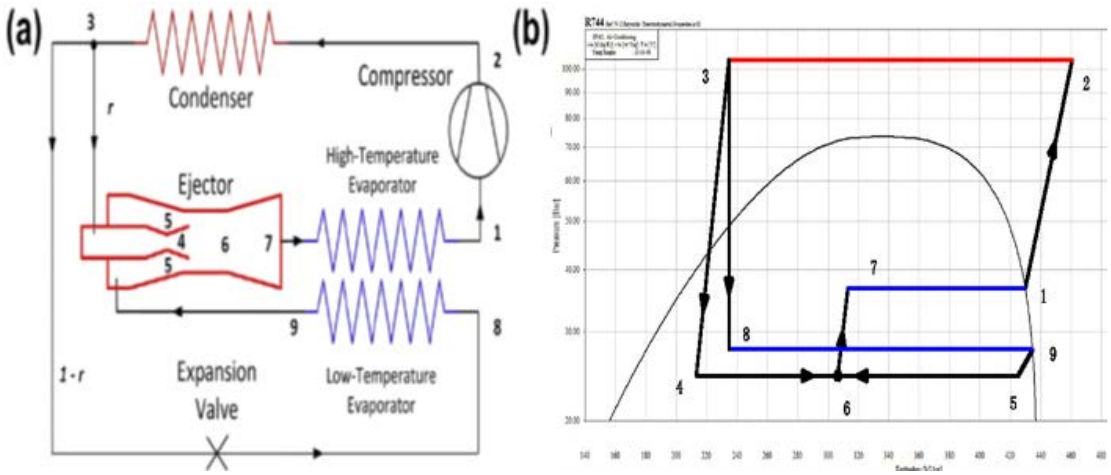

Figure 10 Oshitani cycle layout and corresponding pressure enthalpy diagram (Modified from Lawrence and Elbel, 2013)

3.5 Summary of this chapter

In this chapter, the ejector theory and description of cycles are introduced. At first, the working principle of ejector is introduced. Then, the definition of ejector performance (ejector efficiency) which this paper uses are demonstrated. At last, the description of Gay cycle, Burk cycle and Oshitani cycle are shown. These three cycles are the cycles this paper mainly focus on.

4. Experimental methods and test facility modification

4.1 Description of the test facility and the modification

There are two test facilities involved in this thesis work. The first one is to give the overall view of the ejector performance. And the other one is to compare two systems performance using this ejector. That is to say there are two separate experiments with different objective, but these two experiment are closely related to each other, the first experiment is the prerequisite to the later one.

4.1.1 The ejector performance test facility

The ENEX long ejector is installed in the multi-ejector test rig. In order to install the ENEX ejector, there are some modification work done on the ejector. And the modification and installation work are done at the middle of December 2014. And because of this test rig cannot provide two different evaporation temperature, the objective of using this test rig is to map the efficiency of the new ejector. For further work, this new ejector will install in another test rig.

This test rig is a R744 ejector refrigeration system, and it contains three modules: the R744 unit, the glycol module and the electrical cabinet. This test rig consists of the R744 unit that is together with two auxiliary glycol loops which can provide heat and cooling to the evaporator and the gas coolers. And it can be seen in the following picture. The R744 unit is on the left hand and the glycol unit is on the right hand.

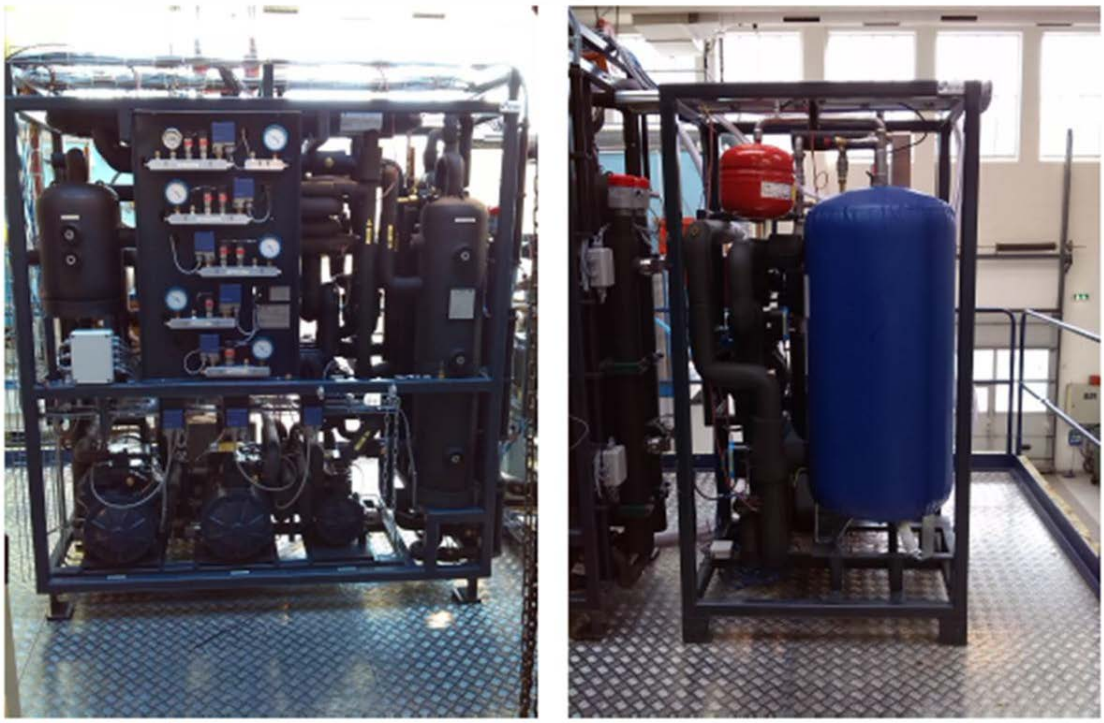

Figure 11 The R744 unit and the glycol unit

And there is a second glycol loop located in the basement. It can provide extra cooling for the system. And this loop is used to decrease the temperature of the ejector's motive nozzle inlet, when the higher temperature loop cannot do it. This loop can see in the following picture.

Figure 12 the second glycol cooler

The next figure shows the modification of the test rig. The ejector is installed parallel to the original ejector housing. In this way, the modification can be done very quickly. It does not affect the original test rig very much. When the experiment is done, the test rig can easily come back to the initial situation.

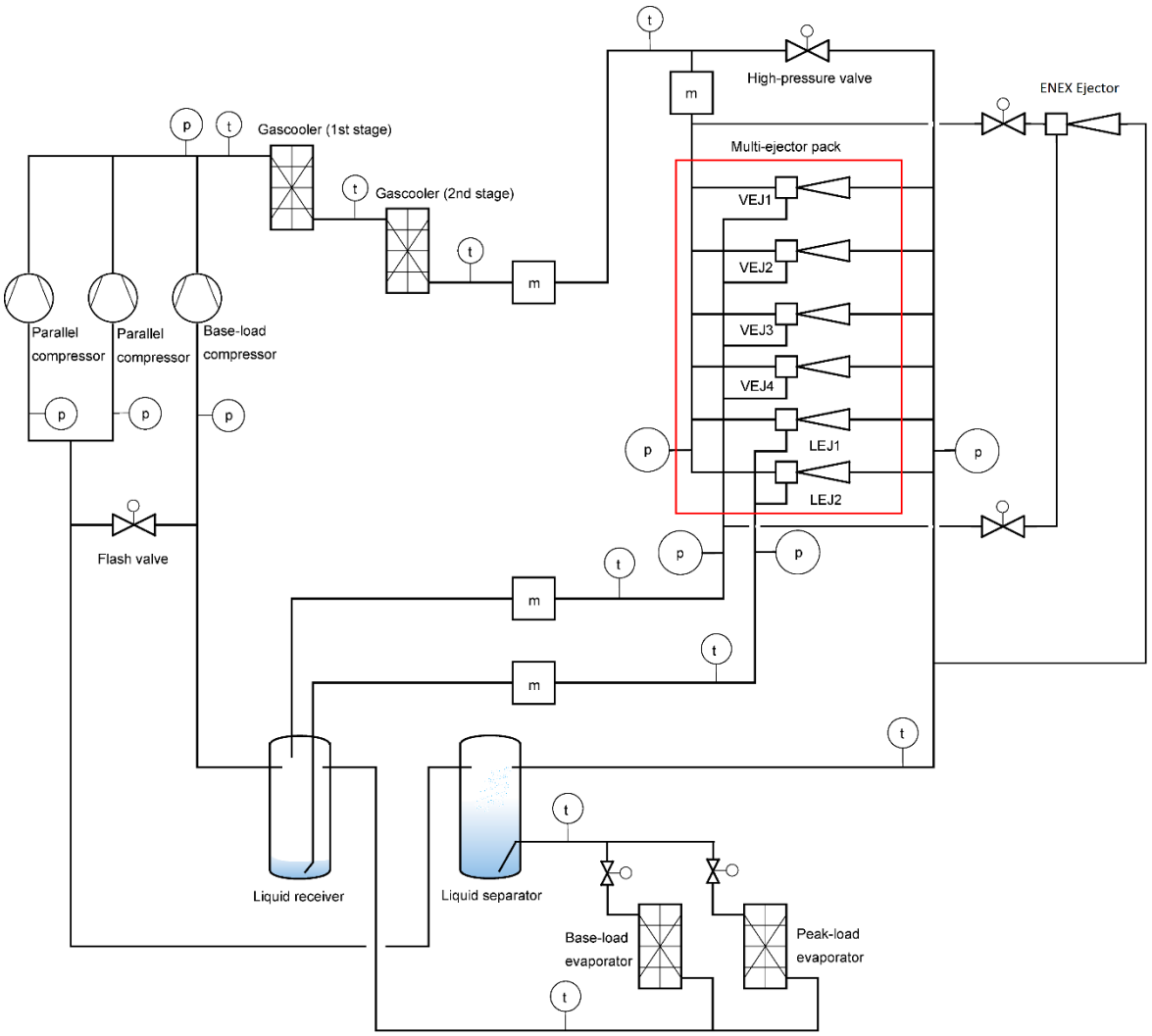

Figure 13 the modification of the test rig

A simplified piping and instrumentation diagram of the R744 system is shown in figure 13. And how the ENEX ejector is installed to this system is showed in figure 13. There are three compressors: one MT compressor and two parallel compressors. And they are with different power capacity operating with two different pressure levels. The MT compressor is connected to the suction accumulation tank, and the two parallel compressors are connected to the liquid receiver. However this system can run only with the MT compressor. In this case, the

flash valve between the MT compressor and the parallel compressors can maintain the pressure difference of the suction accumulation tank and the liquid receiver. This flash valve can also use to keep the desired pressure difference. And it can be seen in the figure an expansion valve that is to protect the system from high pressures. There are two valves to control the the ENEX ejector. One is in the inlet of the motive nozzle, anther is in the inlet of the suction nozzle. When the ejector is working, these two valve should open.

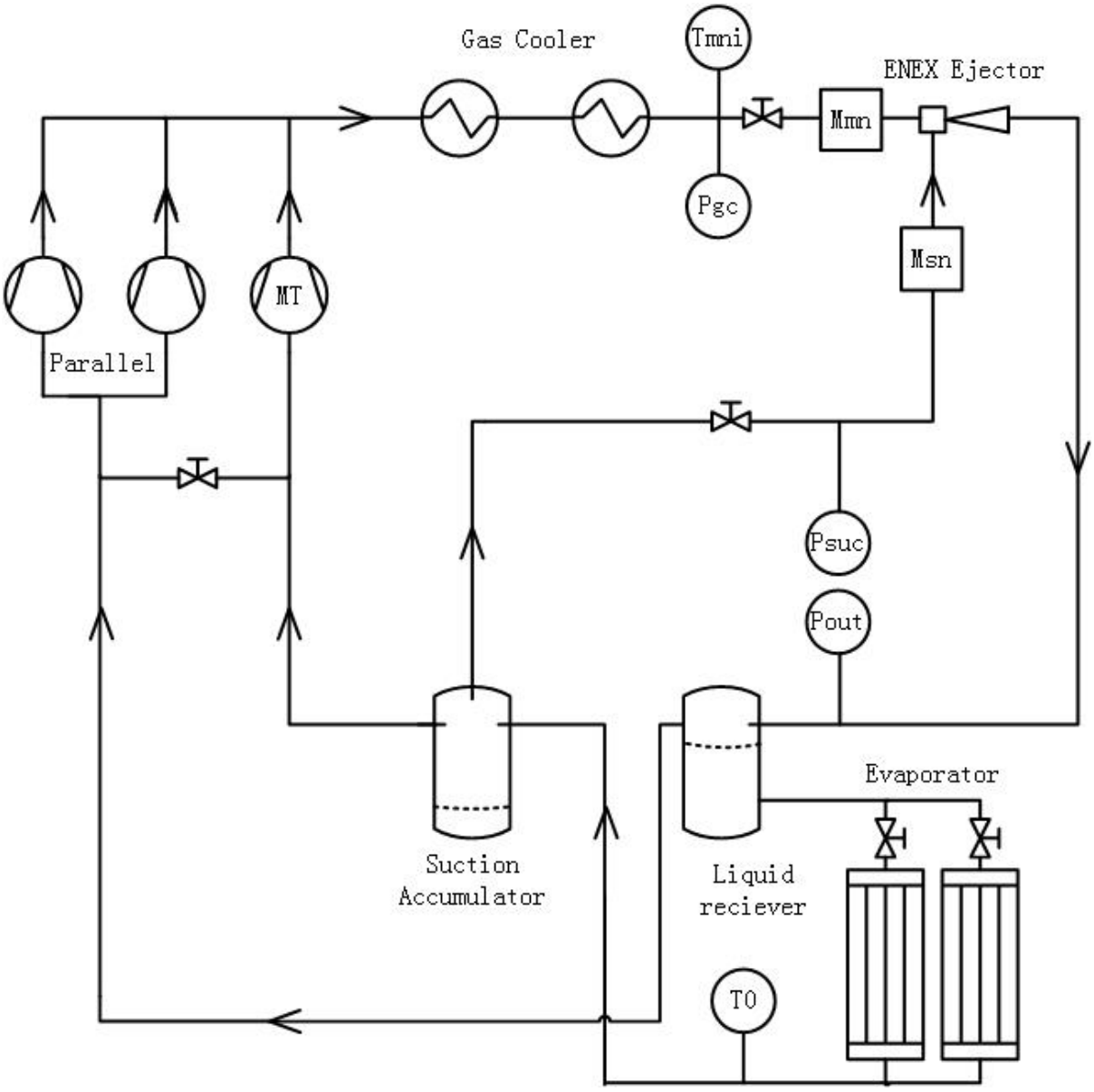

Figure 14 Simplified overview of the experimental R744 system and the installation of the ENEX ejector. The temperature sensors, pressure sensors and mass flow meters (MFM) used to evaluate the ejector experiments are also shown. In this figure non-essential features for the description of the ejector cycle are left out (oil recovery system, different sensors etc.).

The ENEX ejector shows in the next figure. It has two valves to control the motive inlet and the suction inlet. It is installed parallel with the old ejector block.

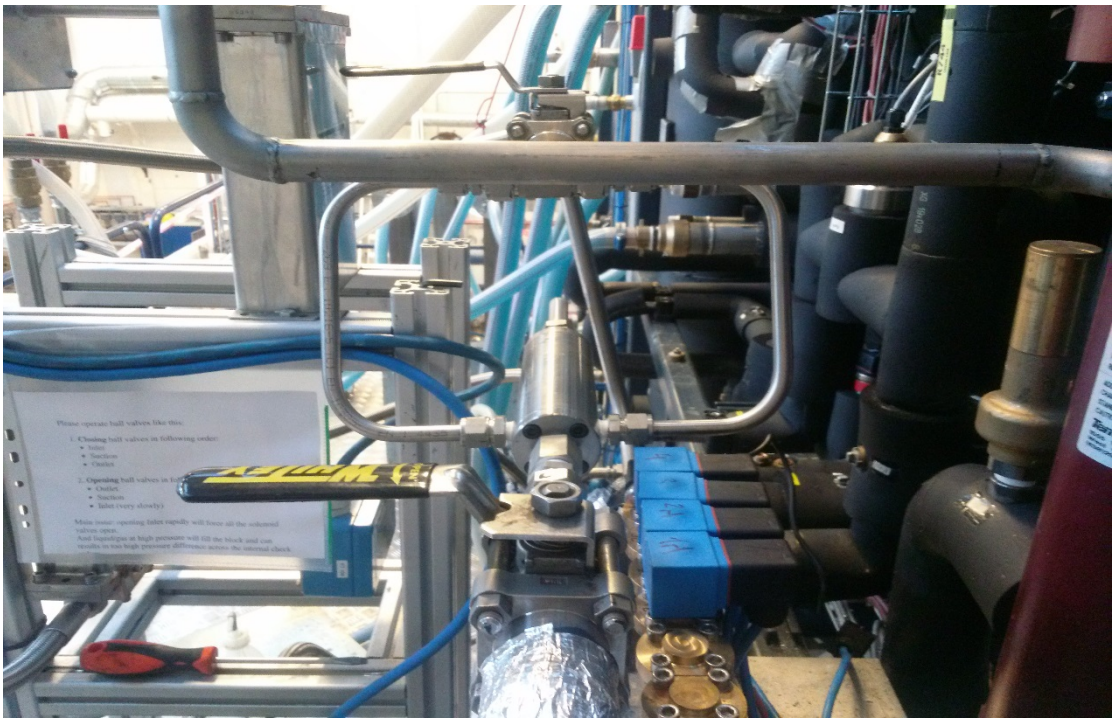

Figure 15 ENEX ejector's installation

There are two auxiliary loops that can see in the next figure. These loops can provide and reject heat to the gas coolers and evaporators. One glycol loop is for removing heat from gas cooler 1 and providing the same heat to the evaporators too. Another low temperature glycol loop is for removing the heat form the gas cooler 2. This loop is located in the basement. There is also an electrical heater located in the glycol tank to provide heat to evaporators. Besides, the glycol can be precooled in an internal water loop in the gas cooler 1.

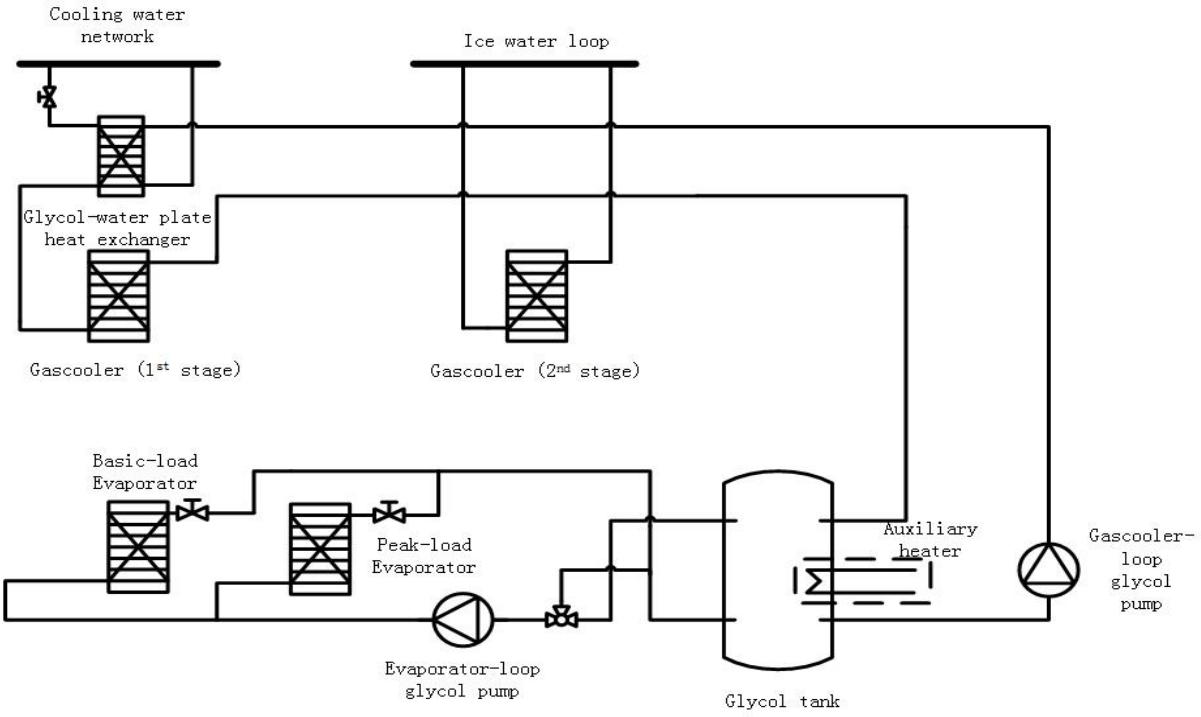

Figure 16 The glycol loops

The main components of the test facility are presented below. The compressors are presented in table 1, and the heat exchangers are presented in table 2. Table 3 shows the magnitude of temperature and pressure sensors used, as well as the accuracy. The sensors are all connected to the Danfoss controller, and every one of them has a purpose in controlling, monitoring and safeguarding the system.

Table 2 Compressors

Component	**Manufacturer**	**Type**
Compressor MT	DORIN	CD 1400 H
Compressor Par 1	DORIN	CD 1000 H
Compressor Par 2	DORIN	CD 360 H

Table 3 Heat Exchangers

Component	**Manufacturer**	**Type**
Gas Cooler 1	KAORI	30 - Plate HX

Gas Cooler 2	KAORI	20 - Plate HX
Evaporator 1	KAORI	30 - Plate HX
Evaporator 2	KAORI	10 - Plate HX
Water Loop	KAORI	10 - Plate HX

Table 4 Sensors and instrumentation installed to monitor the test facility

Instrument	Brand	Product ID	Type	Description/ Location	Accuracy of Reading
Pressure	Danfoss	AKS 2050	Pizoelectric	R744	± (0.3%)
Temperature	Danfoss	AKS 21 A	PT1000	R744 and Glycol	± (0.3 + 0.005 · *T*)
Mass flow	RHEONIK	RHM06	Coriolis	R744	± (0.2%)
Mass flow	RHEONIK	RHM15	Coriolis	Glycol	± (0.2%)

All sensors are connected to the Danfoss control unit. The controller then processes and transmits selected signals live to the Danfoss Minilog system, a software running on the operator computer. The process of the software is shown in the next figure. The operator is able to change different setting points (evaporator temperature, gas cooler pressure, gas cooler temperature) . The Minilog system uses graphical representation of the key-parameters, enabling an easy way of monitoring multiple parameters simultaneously.

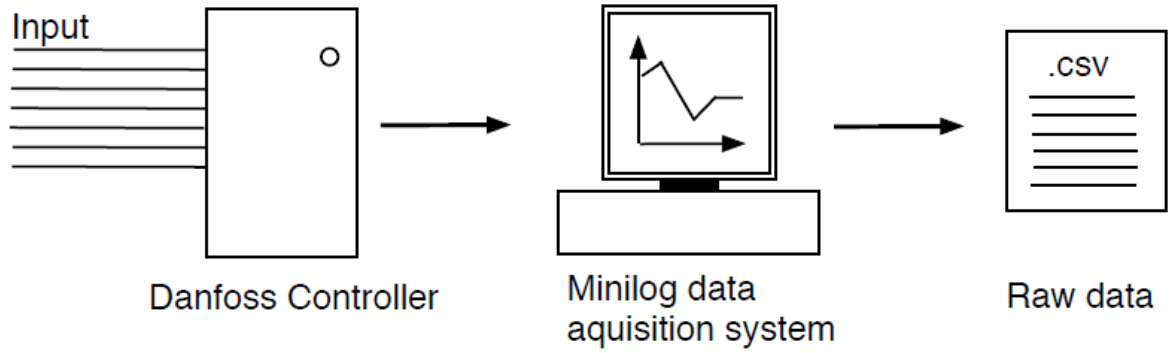

Figure 17 Data acquisition procedure

From the Minilog system, data is recorded and exported. When a given test condition

was reached steady state, operation was determined, the test point was recorded. The duration of the recording was set to six minutes to minimize the influence of minor oscillations, and ensure that the time constants in the system was accounted for (constant heat conduction, mass flow rate etc.). Data from the Minilog system was then exported to .csv-files and imported in a post processing Excel spreadsheet created specifically for this purpose. Due to the number of points recorded, a program was developed in the Visual Basic environment to fully automate the processing of each test point in which REFPROP 8.0 was used for thermodynamic properties. The spreadsheet calculated ejector efficiency, mass entrainment ratio, and pressure lift, along with both type A and B uncertainties (uncertainty definitions are presented in next chapter). An additional excel spreadsheet was also created in order to gather data from every processed point, with the aim of creating day to day reports, or export data for plotting in third party software. The structure of the post processing is shown in next figure.

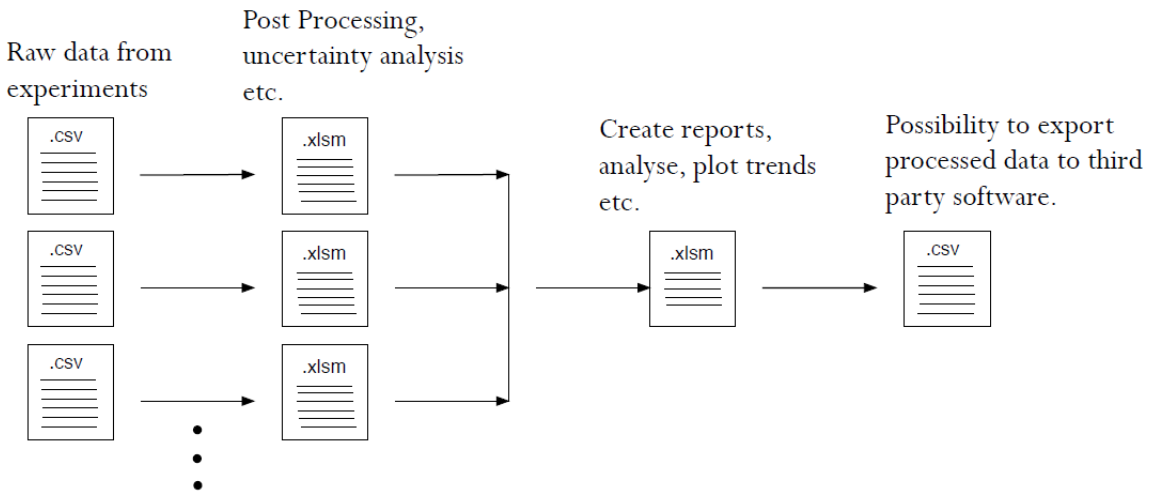

Figure 18 Data processing procedure

4.1.2 The systems' performance test facility

The test facility used to compare the two systems is placed in NTNU / SINTEF laboratory in Norway (Trondheim). Simplified overview of this test rig and the installation of the ejector is shown in figure. Panoramic view of the test rig is presented in figure, and together with this test rig there are some auxiliary loops which are not shown in this picture are placed in the basement.

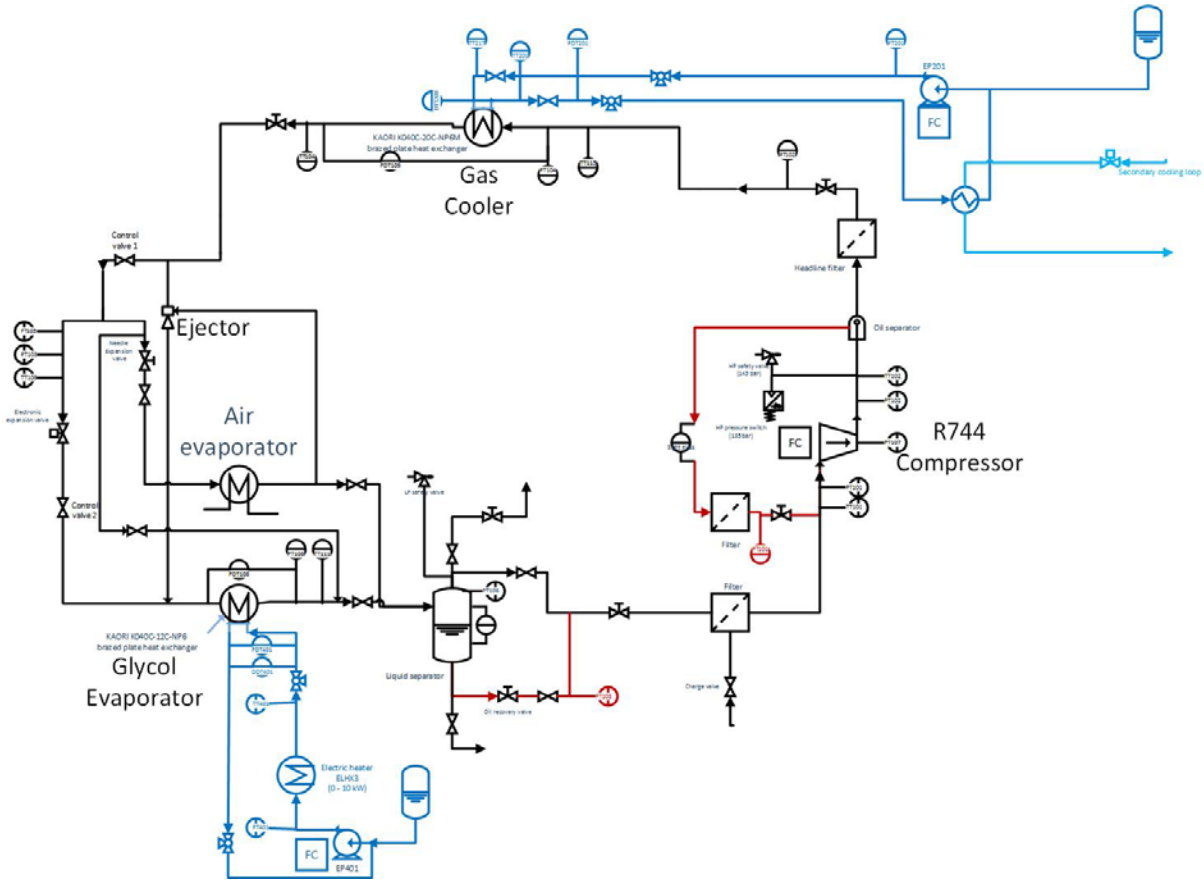

Figure 19 Simplified overview of the test rig and the installation of the ENEX ejector.

Figure 20 Panoramic view of the test facility

The system includes a compressor, gas cooler, ejector, and two evaporators. There are many valves that can control the system working as the Condenser Outlet Split system or the

Diffuser Outlet Split system. A brief description of each component is located in following section.

The CO_2 compressor C99-5 with variable displacement manufactured by OBRIST is used in the test rig. Maximum refrigerant mass flow, maximum high pressure and maximum outlet temperature are 400 kg/h, 140 bar and 160 ℃ respectively. And the rotational speed of the compressor is in range of 600-6000 rpm.

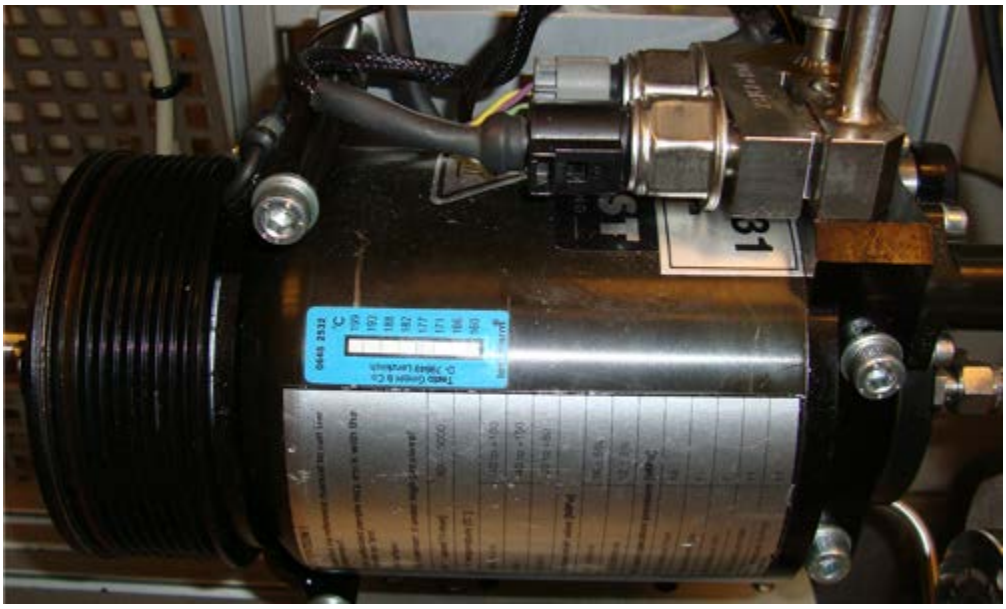

Figure 21 The CO_2 compressor C99-5 with variable displacement

The ejector is ENEX long ejector which is the very ejector used in the experiment before. The ENEX ejector was installed parallel to the existing expansion devices by use of various certified components of the existing system. Technical attachments have done including technical drawing of the ENEX ejector and update of the P&ID diagram.

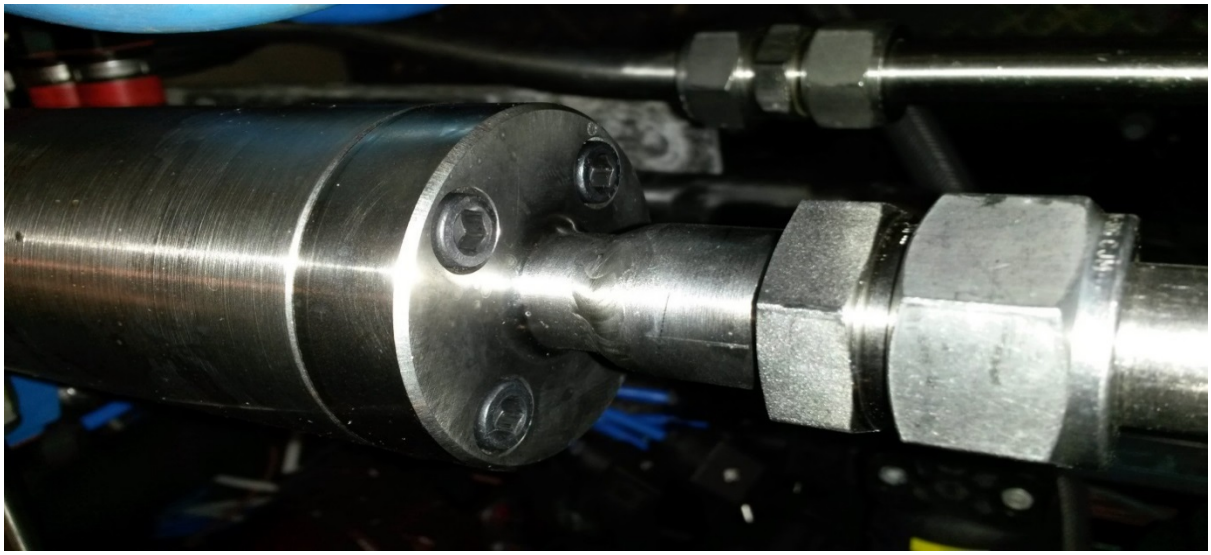

Figure 22 The ejector

In this system, we use two evaporators in order to provide two different evaporation temperature. The first evaporator is air cooled evaporator used as low temperature evaporator. There is an air fan to control the air flow rate. The other one is glycol cooled evaporator used as high temperature evaporator. There is also a glycol pump to control the glycol mass flow. Later the load of these evaporator can calculate by the air and glycol side respectively.

The measurement devices' properties are showed in next figure with the uncertainty of each of them.

Table 5 The measurement devices' properties

Instrument	Range	Uncertainty
Thermocouple (THERMOCOAX, Cu/CuNi)	-200 to 350 ℃	± 0.3 K
Pressure transmitter	7 to 14 MPa/1 to 7 MPa	± 0.075 % max range
Differential pressure tansmitter	-0.5 to 1 MPa	± 0.075 % max range
Mass flow meter	0.2 to 10 kg/min	± (0.2%)

T-type thermocouples installed in the test rig were made by THERMOCOAX Company. For proper working condition, it is important to use it to measure temperature in range from -200 to 350 ℃. Pressure transmitters used in research were made by Endress + Hauser Company. Very good reproducibility and long-term stability guarantee good quality and reliable

results.

To measuring absolute pressure in the range of 7 to 14 MPa, PDT75 type sensors were used and for differential pressure from -0.5 to 1 MPa, PMP71 type. All transmitters were calibrated and a linear equation for the pressure-signal relation was determined. Mass flow meters for CO2 and for water/glycol were made by RHEONIK Company. They were Coriolis type meters with the repeatability around 0.1 per cent specified by the manufacturer.

The software that user can control the system is built on Lab-view. This software helps non-programmers to project programs by dragging and dropping virtual representation of lab equipment. In the next figure, the example windows on the lab is shown. Logging process, which is schematically presented in Figure saved all data read from thermocouples, pressure sensors, flow meters etc. to the Microsoft Excel file.

To process the rough data, a new Excel is made basis on the old Excel made by the former user. It takes a lot to enter all the equations and formula that needed to process the rough data. The uncertainty calculation also insert to the Excel file. The Excel file has three main part: COP calculation, uncertainty calculation and exergy analysis. When the file is finished, it is a comfortable experience to process the data. This file uses Rnlib library to calculate values of thermodynamic parameters and presents all important results in user-friendly interface. RnLib is a separate function for Excel. It basically adds formulas to the existing Excel formulas. RnLib was developed by SINTEF. It can calculate in an Excel sheet enthalpy, entropy, etc. for given refrigerants, temperatures and/or pressures. This treatment gives fast preliminary view on results from one logging data process.

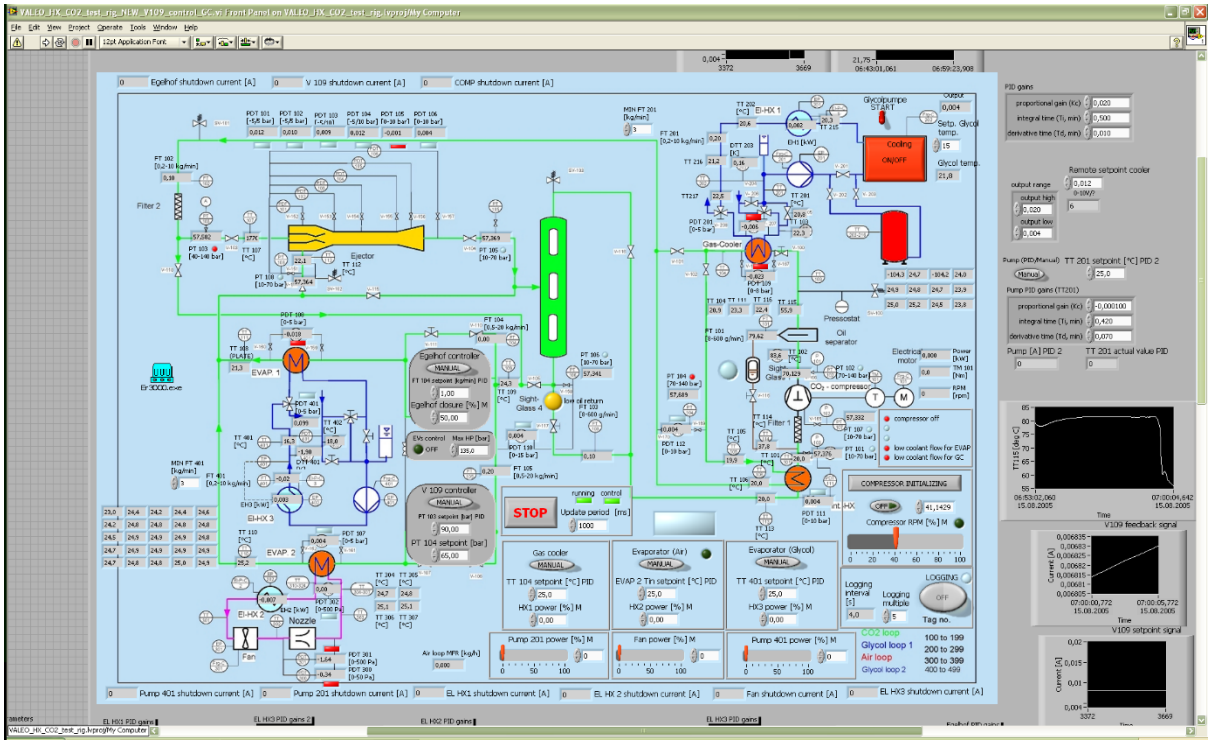

Figure 23 System control panel

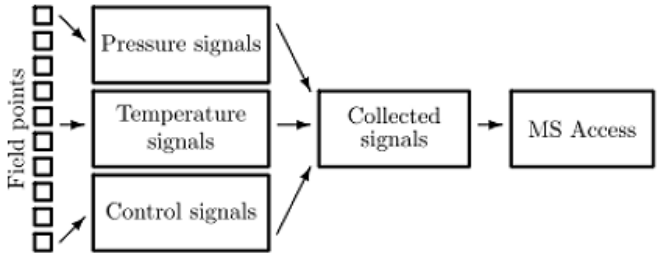

Figure 24 Scheme of logging process

4.2 The plan to do the experiment

4.2.1 Overall view of the ejector performance

The objective of first experiment is to give a better understanding of the ejector performance, and it is a preparation to do the next experiment. The control of the ejector refrigeration system gives a lot of different parameters, but the most important parameters are the following:

The evaporation temperature (T_0): because of the time is limit, so the study has been carried out for on temperature, and it is around -8 degrees centigrade.

The motive nozzle inlet temperature (T_{MNI}): the ejector behavior has been analyzed for a range of temperatures between 21 and 33 degrees centigrade. The inlet of the motive nozzle temperature is not too low in this case, so the auxiliary low temperature loop is not used.

The discharge pressure (P_{GC}): the discharge pressure is set in auto model, and it is from 6 MPa to 8 MPa approximately.

The ejector outlet pressure (P_{OUT}): The ejector outlet pressure is set from 3 MPa to 3.7 MPa approximately, and one step increases one bar, until there is no suction flow.

The pressure lift (ΔP): the pressure difference between the liquid receiver and the suction accumulator.

The suction mass flow ($\dot{m}_{SN}$) and the motive mass flow ($\dot{m}_{MN}$): the mass flow of the suction nozzle and the motive nozzle.

It can see in the next table, all the set points which have been operated by the ejector refrigeration system in the test facility. The ejector is tested within these test points, then the performance map of the ejector can be acquired through the test.

Table 6 Test points of ejector performance

Test points	Point 1	Point 2	Point 3	Point 4	Point 5	Point 6	Point 7
T_{MNI}/°C	19	20	21	22	23	24	25
P_{GC}/MPa	6	6	6.5	6.5	6.5	6.5	7
Test points	Point 8	Point 9	Point 10	Point 11	Point 12	Point 13	
T_{MNI}/°C	26	27	28	29	30	31	
P_{GC}/MPa	7	7.5	7.5	8	8	8	

In order to explain the ejector performance, we need to show several parameters, such as the mass entrainment ratio of the ejector, the pressure ratio and the ejector efficiency.

The mass entrainment ratio (ϕ) is the ratio of the suction mass flow rate ($\dot{m}_{SN}$) to the motive mass flow rate ($\dot{m}_{MN}$):

$$\phi = \frac{\dot{m}_{SN}}{\dot{m}_{MN}} \tag{4-1}$$

The pressure ratio (Π) is the ratio of the ejector suction pressure (P_{SUC}) to the ejector outlet pressure (P_{OUT}):

$$\Pi = \frac{P_{OUT}}{P_{SUC}} \tag{4-2}$$

The ejector efficiency (η) has talked before in chapter 3:

$$\eta_{ejector} = \frac{\dot{W}_{rec}}{\dot{W}_{\max\ rec}} \tag{4-3}$$

4.2.2 Comparison of the different systems

The comparison between COS (condenser outlet split) and DOS (diffuser outlet split) systems is done in this experiment. There are two valve that are very important to control the system to run as COS or DOS system. When the control valve 1 is open and the control valve 2 is closed, the system runs as COS system. Otherwise, the system runs as DOS system. The fig below shows how the control valve works.

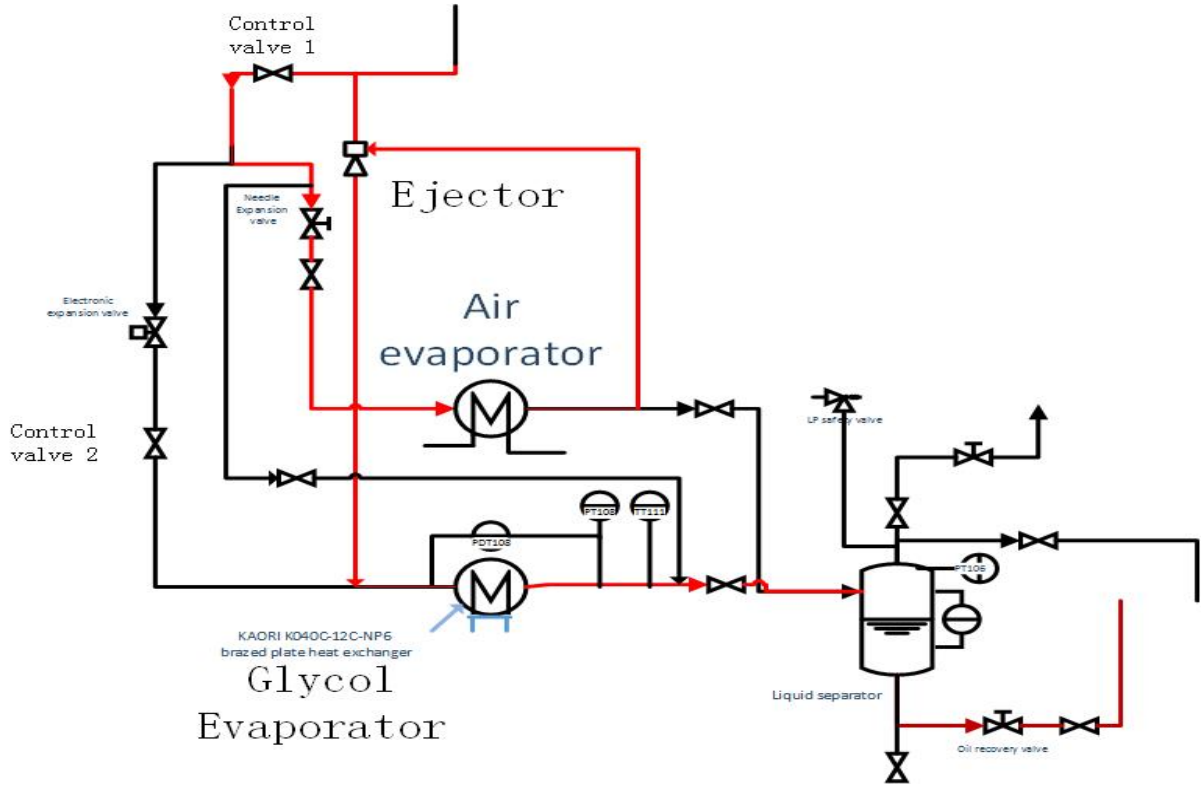

Figure 25 COS system

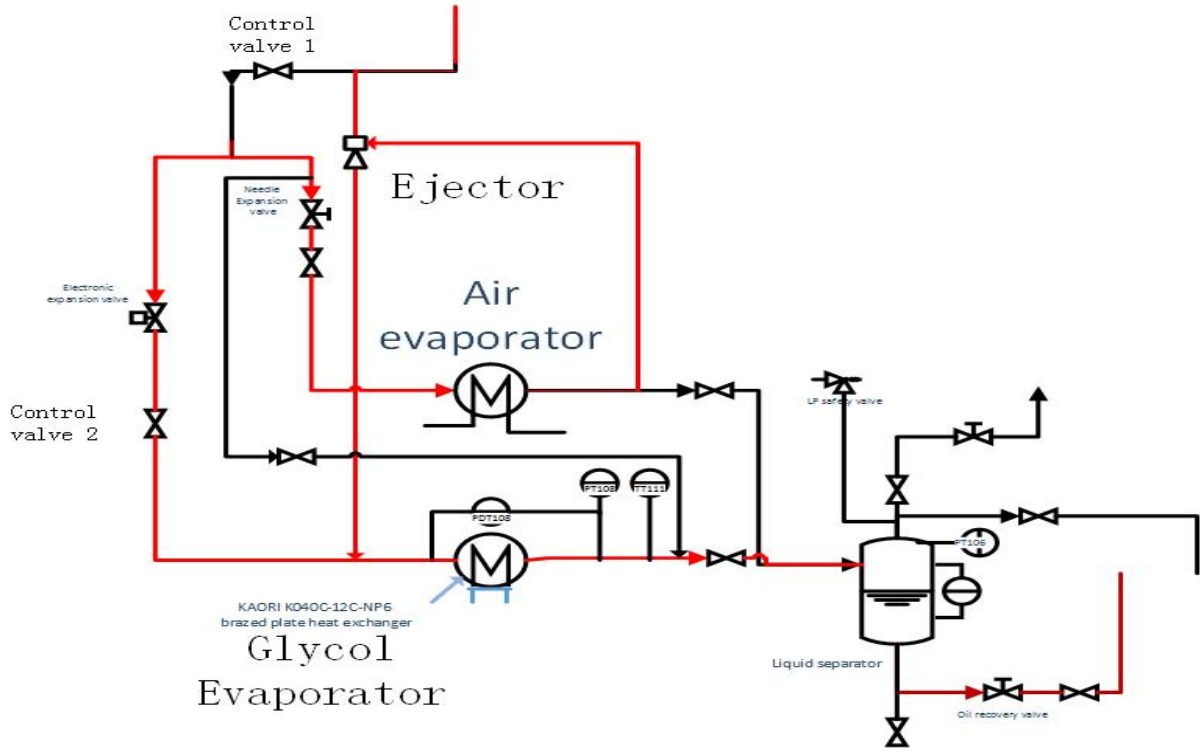

Figure 26 DOS system

The most difficult part in this plan to set the temperature of the glycol evaporator and air evaporator. Because, these two temperature should have some meaning in real life. That is to say the evaporator can working for some real life purpose. But due to the compressor capacity is limit and the system is not optimized, the temperature of two evaporator cannot just set to some certain value. So some pre-experiments are done to figure out the value setting in this experiment.

In the experiment, the two system's refrigerant load remains the same, through setting the opening degree of the glycol pump and fan for cooling the two evaporator, the inlet and outlet temperature as the same. The opening degree of glycol evaporator pump is 23%, and the fan is 43%. The inlet and outlet temperature of glycol evaporator is 20℃ and 8℃ respectively. For air evaporator is 11℃ and 2℃ respectively. Through adjusting the compressor speed and the opening degree of glycol pump for the gas cooler cooling loop, the gas cooler outlet temperature can be set to some certain value. The gas cooler outlet temperature is set from 30 ℃ to the maximum temperature that the compressor is working on full-load.

Table 7 Test points of cycle’s comparison

COS	Point 1	Point 2	Point 3	Point 4	Point 5	Point 6	Point 7
T_{gc}/℃	30	31	32	33	34	35	36
DOS	Point 1	Point 2	Point 3	Point 4	Point 5	Point 6	Point 7
T_{gc}/℃	30	31	32	33	34	35	36

4.3 Summary of this chapter

This chapter focus on the experimental methods and the test facility modification. There are two test facilities involved in this thesis work. The first one is to give the overall view of the ejector performance. And the other one is to compare two systems performance using this ejector. That is to say there are two separate experiments with different objective, but these two experiment are closely related to each other, the first experiment is the prerequisite to the later one. These two experimental methods and test facility modification are introduced on this chapter.

5. Experimental analysis

5.1 overall view of ejector performance

There are two main parameters, which are the motive nozzle inlet temperature (T_{MNI}) and the discharge pressure (P_{GC}). All the test points can be found in the appendix. And a lot of specific data are recorded in the appendix, also with some graphics.

The ejector efficiency represents as a curve with the pressure ratio is raising. The maximum of the efficiency show up in the middle of the curve. This is because the friction losses generated into the ejector reach its minimum for the respective pressure ratio depending on the motive inlet temperature. As it can be seen in the next figure:

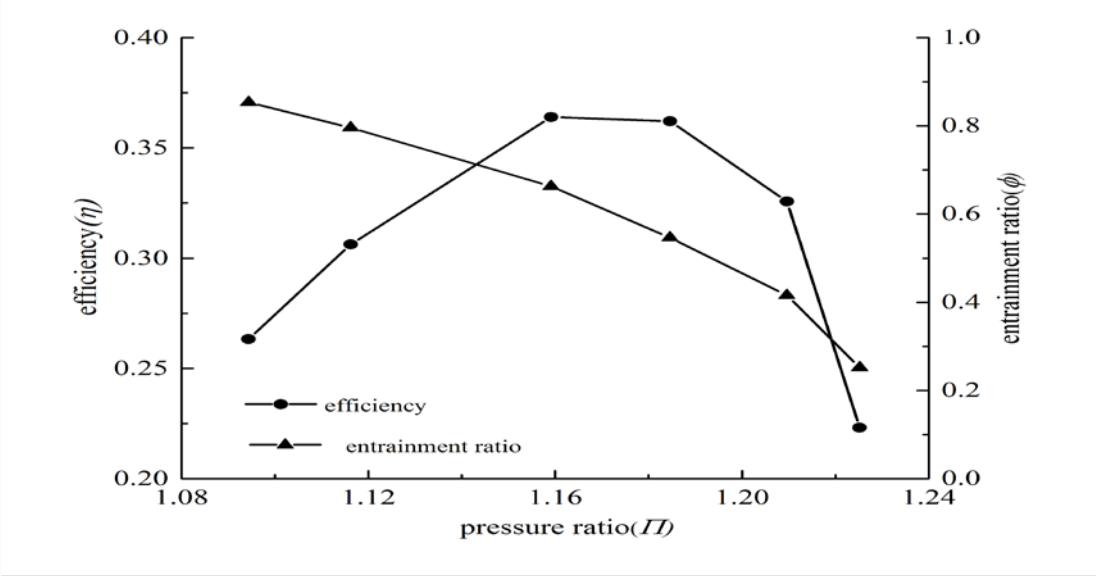

Figure 27 The relation between efficiency, entrainment ratio and pressure ratio

In this test point, the motive inlet temperature is 30℃, the discharge pressure is 8 MPa approximately and the evaporation temperature is -8℃ . In this relatively high motive inlet temperature, the performance of the ejector is quite good and the maximum efficiency can reach 0.37 when the pressure ratio is 1.16. As it can be seen in the figure, the entrainment ratio decreases when the pressure ratio increases. Because the discharge pressure is more or less steady, it can be concluded when the receiver pressure increases, the entrainment ratio decreases. And when it comes to efficiency of the ejector, the maximum efficiency shows up at the moderate pressure ratio and the moderate entrainment ratio.

Because there are too many parameters related to the performance of the ejector, it is necessary to use a 3D graphic to show how the efficiency is related to these parameters. By using a graphic software named Origin, these parameters can represent in 3D dimensions, and the different axis are the discharge pressure (P_{GC}), the motive inlet temperature (T_{MNI}) and the pressure ratio (Π). It can also represent the efficiency of each test point by using different ranges of colors. In figure 17, it can easily see that the high efficiency can be achieved in the medium pressure ratio with respective discharge pressure, and with the motive inlet temperature raising the higher efficiency show up in higher pressure.

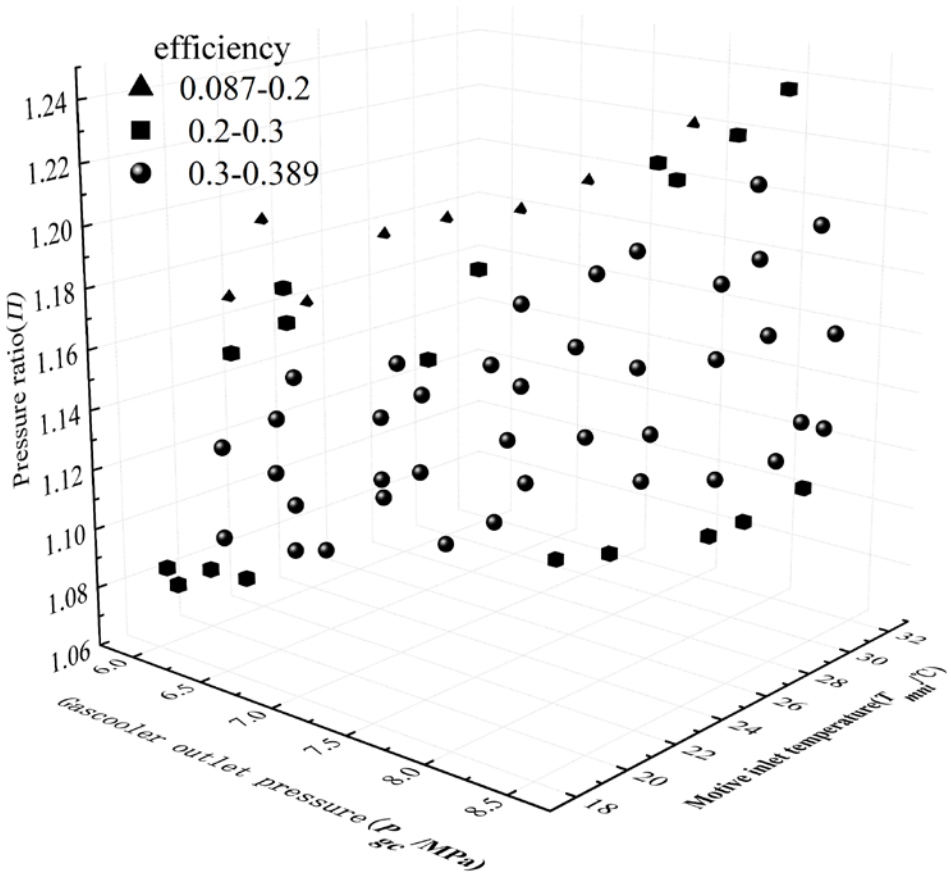

Figure 28 3D representation of all test points' efficiency

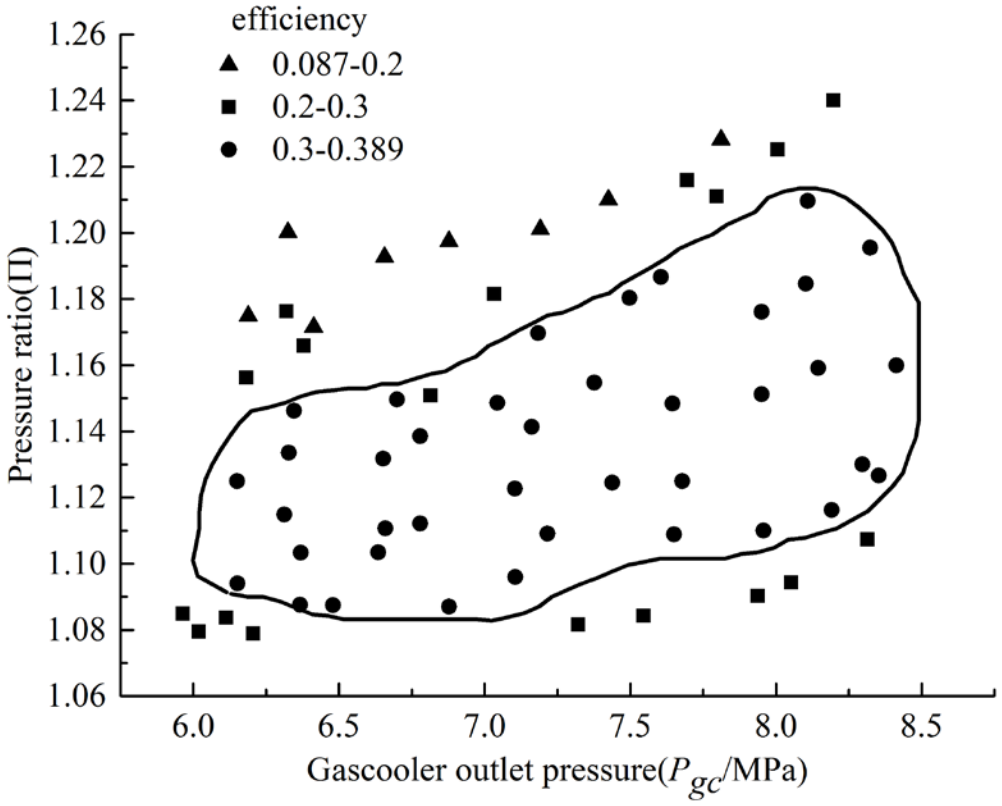

Figure 29 The relation between pressure ration, discharge pressure and efficiency

In figure 29, it can see clearly with the discharge pressure raising, the high efficiency can be achieve at moderate pressure ratio, and the pressure ratio range is from 1.09 to 1.20 approximately. That is to say, the ejector can achieve at high efficiency at large range of discharge pressure, and with the appropriate pressure ratio. In the envelop, the efficiencies of ejector are all above 0.3 except one point is 0.297 which is also a high efficiency, the motive inlet temperature is from 20 to 30 ℃.

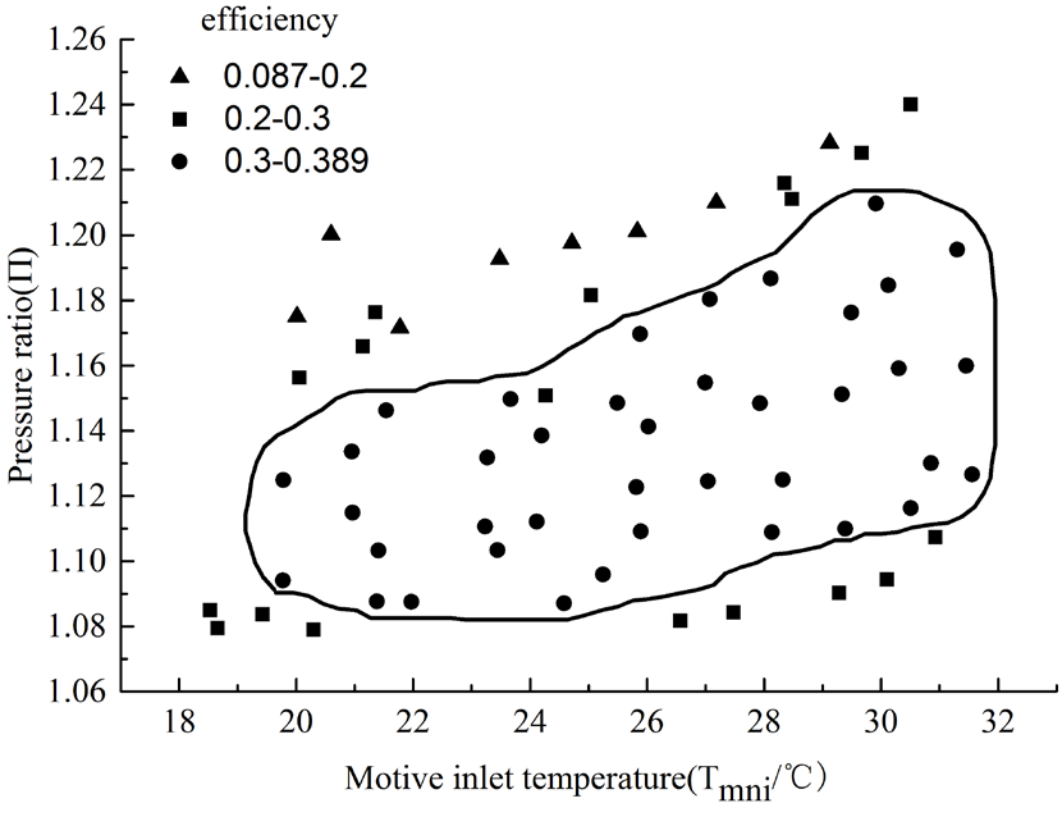

Figure 30 The relation between pressure ratio, motive inlet temperature and efficiency

In figure 30, it can see clearly with the motive inlet temperature increasing, the high efficiency can show up at moderate pressure ratio, just as it is said before. When the pressure ratio is too high, the efficiency can be very low. So when the ejector is in operation, this situation should be avoided. In the envelop, the efficiencies of ejector are all above 0.3 except one point is 0.297 which is also a high efficiency, the gas cooler outlet pressure is from 6 to 8 MPa.

In figure 31, it can see the ejector works more efficiently when the entrainment is from 0.4 to 0.8 approximately. And the pressure ratio is from 1.08 to 1.22. That is to say when the entrainment is too low or too high the ejector does not work well due to with no mass flow the ejector cannot reduce the energy consumption and with too much suction flow the ejector cannot work well. In the envelop, the efficiencies of ejector are all above 0.3 except one point is 0.297 which is also a high efficiency, the motive inlet temperature is from 20 to 30 ℃ and the gas cooler outlet pressure is from 6 to 8 MPa.

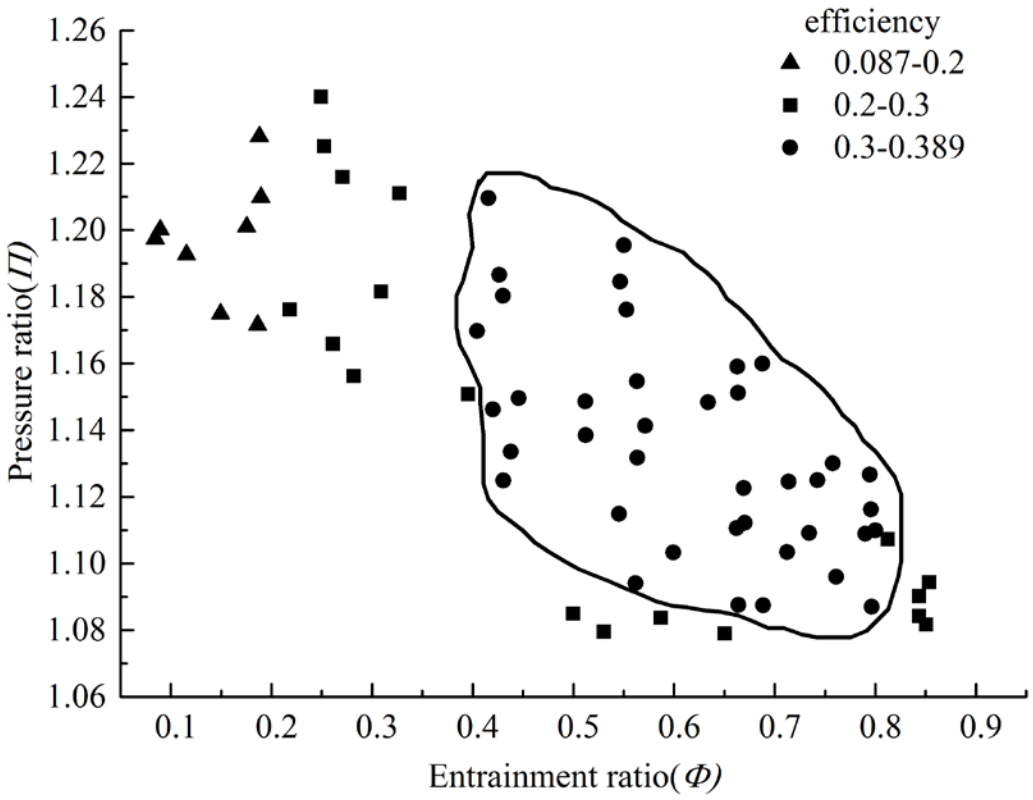

Figure 31 The relation between entrainment ratio, pressure ratio and efficiency

Nevertheless, the recorded values of the motive nozzle mass flow rate can approximate by use of mathematic formula:

$$\dot{m}_{MN} = \frac{\pi}{4} {d_{th}}^2 (A{\rho_{in}}^2 + B\rho_{in} + C\left({p_{in}}/{p_{cr}}\right)^2 + D\,{p_{in}}/{p_{cr}} + E) \qquad (5\text{-}1)$$

Where:

$\dot{m}_{MN}$-motive nozzle mass flow rate, kg/s

d_{th}-motive nozzle throat diameter, m

ρ_{in}-motive nozzle inlet density, kg/m^3

p_{in}-motive nozzle inlet pressure, Pa

p_{cr}-critical pressure for R744, 7377300 Pa

A, B, C, D, E-coefficients adjusted individually

Table 8 Coefficients in Eq. (5-1) and deviation between the measured and approximated mass flow rate

A, $m^4/(kg \cdot s)$	B,m/s	C, $kg/(s \cdot m^2)$	D, $kg/(s \cdot m^2)$	E, $kg/(s \cdot m^2)$	Relative deviation range
-4,76117E-01	8,18031E+02	6,88151E+04	-9,68003E+04	-2,84328E+05	+3,32 % -3,71%

The approximation function should be strictly limited the area the experimental work performed. Thus, extrapolation may generate much higher deviation.

In addition, the suction performance can approximate by functions below:

$$\dot{m}_{SN}/\dot{m}_{MN} = A_1(p_{DIF,out}/p_{SN,in})^2 + A_2\, p_{DIF,out}/p_{SN,in} + A_3 \quad (5\text{-}2)$$

Where parameters define as below:

$$A_i = (a_{i,1}{\rho_{MN,in}}^2 + a_{i,2}\rho_{MN,in} + a_{i,3}\left(p_{MN,in}/p_{cr}\right)^2 + a_{i,4}\, p_{MN,in}/p_{cr})(a_{i,5}\, p_{SN,in}/p_{cr} + a_{i,6}) \quad (5\text{-}3)$$

Where:

$\dot{m}_{MN}$-motive nozzle mass flow rate, kg/s

$\dot{m}_{SN}$-suction nozzle mass flow rate, kg/s

$\rho_{MN,in}$-motive nozzle inlet density, kg/m^3

$p_{MN,in}$-motive nozzle inlet pressure, Pa

$p_{SN,in}$-suction nozzle inlet pressure, Pa

$p_{DIF,out}$- diffuser outlet pressure, Pa

p_{cr}-critical pressure for R744, 7377300 Pa

Table 9: Coefficients in Eq. (5-3) and absolute deviation between the measured and approximated suction nozzle mass flow rate

Coefficient A_i	$a_{i,1}, m^6kg^2$	$a_{i,2}, m^3/kg$	$a_{i,3}, -$	$a_{i,4}, -$	$a_{i,5}, -$	$a_{i,6}, -$	Absolute deviation range
i=1	2.0371E-01	-2.0275E+02	-1.0443E+03	3.3538E+04	-4.6428E-02	2.0072E-02	+0.041 -0.036
i=2	3.3507E-01	-3.3450E+02	-4.8571E+03	5.8794E+04	6.8741E-02	-2.9024E-02	
i=3	1.7136E-01	-1.7245E+02	-5.2386E+03	3.3925E+04	-8.3667E-02	3.4522E-02	

Through the approximation above, a rough relation between mass flow, pressure and density shows that, the experiment data can well fit the approximation. However, beyond the data area, the approximation may have a bigger deviation.

5.2 comparison of the two systems

In this experiment, there are two systems compared: Condenser Outlet Split system and Diffuser Outlet Split system. There are seven test points of each system as the gas cooler outlet temperature raising from 30℃ to 36℃. Gas cooler outlet temperature is controlled by the compressor load and gas cooler' cooling loop glycol pump opening degree. When the compressor RPM increases and the glycol pump opening decreases, the gas cooler outlet temperature increases. Each system has two evaporators: glycol cooled evaporator and air cooled evaporator. The refrigeration load remains same of each system in all the test points. The opening degree of glycol cooled evaporator pump remains 23%, and the inlet and outlet temperature remain

20℃ and 8℃ respectively. The opening degree of air cooled evaporator fan remains 43%, and the inlet and outlet temperature remain 11℃ and 2℃ respectively.

In the next figure, it shows the COP of the two systems. It can be seen the COP is very low. There are several reasons causing the low COP: the whole test rig is not design for the ENEX ejector, the diameter of pipe line is too small for the ejector; The compressor capacity is too small for the ejector which should utilize in bigger system; On the heater exchanger side, the gas cooler and glycol evaporator, there isn't any insulation providing heat leakage. After all, the test rig is not optimized for the ejector is the main reason for the low COP. But the objective of the experiments is to compare these two systems. The two systems' running condition is the same. So the comparison is still useful. The DOS system's COP is much better to COS.

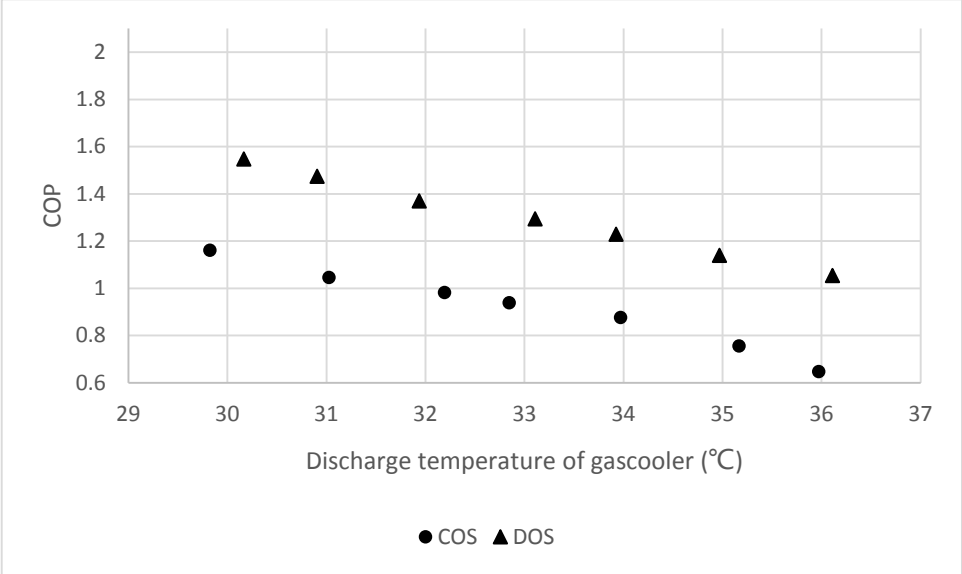

Figure 32 COP comparison between COS and DOS cycle

The percentage increased COP from DOS system to COS system is shown in next figure.

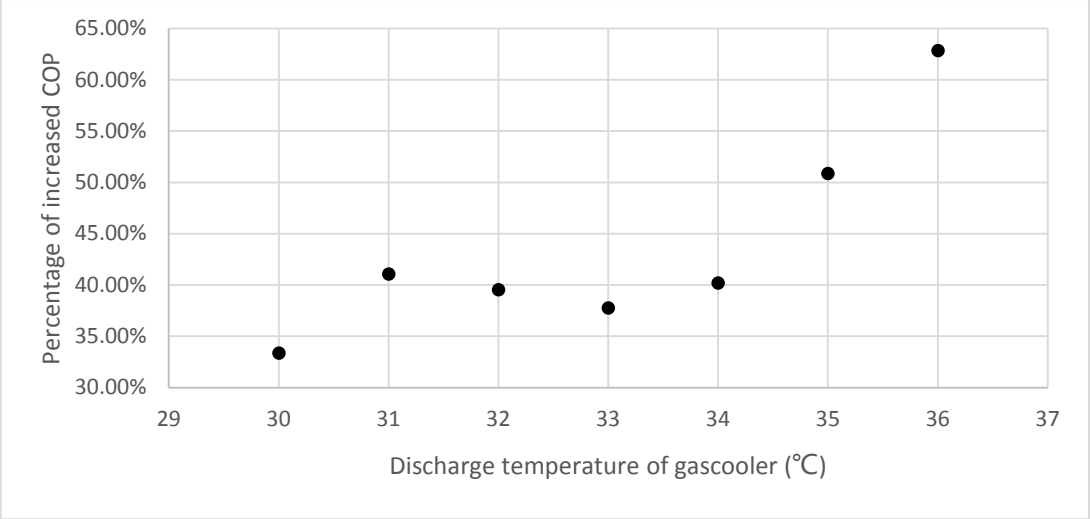

Figure 33 The percentage of increased COP

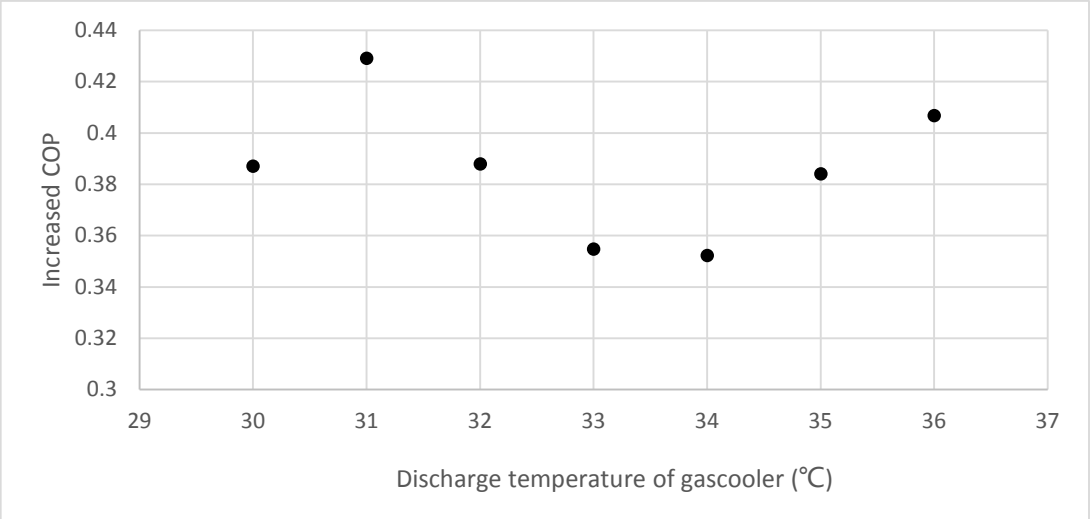

Figure 34 The increased COP

As said before, the pipe line's diameter is too small for the system. So the pressure loss is huge from discharge of compressor to the inlet of the gas cooler, and it is about 10 bar. Compensate calculation of gas cooler discharge side is done and the result shows in the next figure. It shows the two systems' COP are all increased. The DOS system still better than COS system. But the increased COP is less than the real situation. That is to say after compensate of gas cooler discharge pressure loss, the difference between two systems becomes smaller.

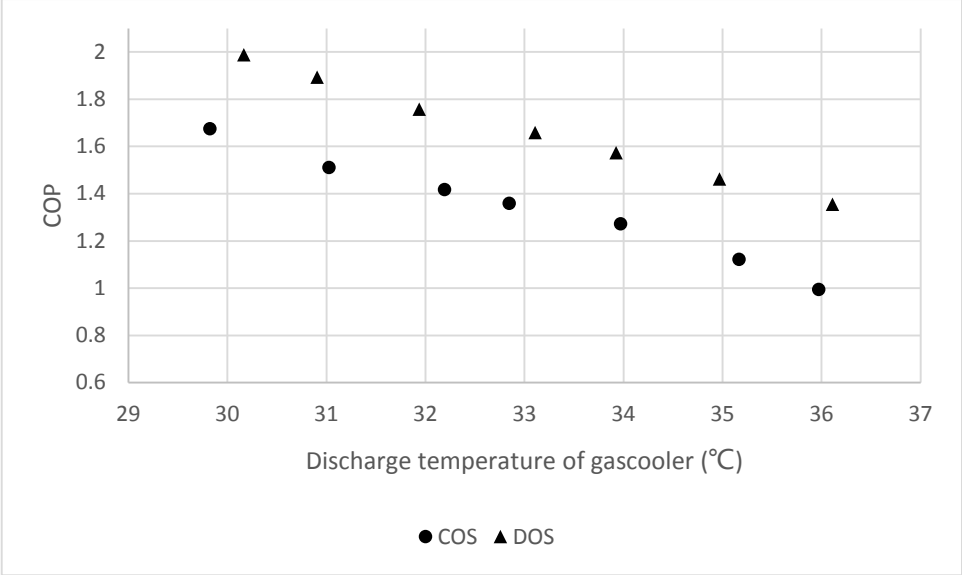

Figure 35 Compensate COP from Compressor discharge Side

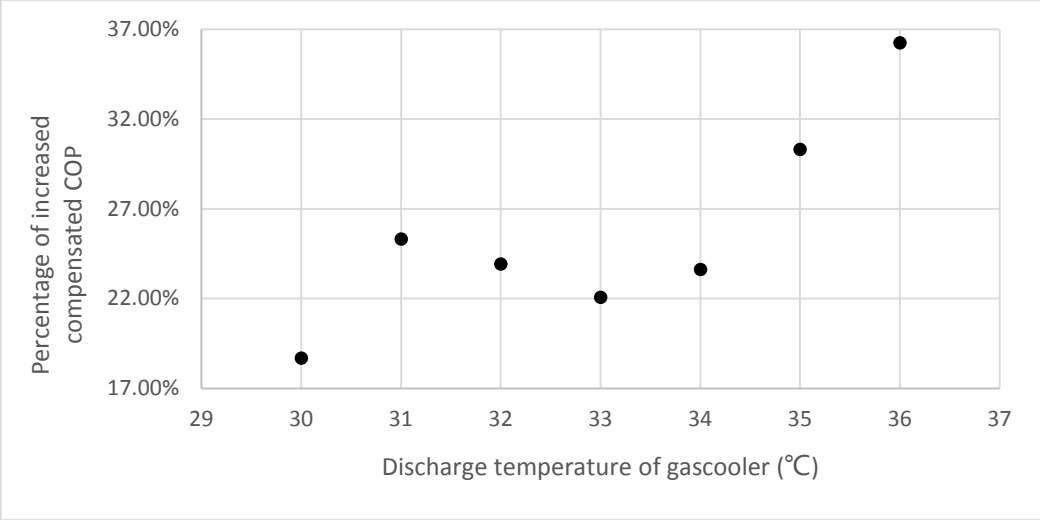

Figure 36 The percentage of increased compensated COP

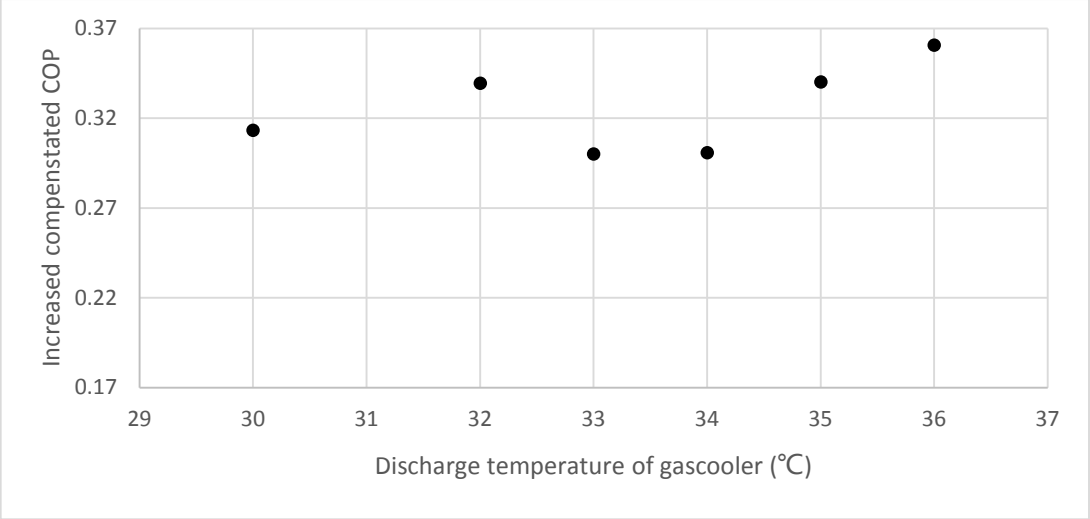

Figure 37 The increased compensated COP

Because the system is not optimized, there is also pressure loss on the compressor suction side. The pressure loss between the glycol evaporator outlet and the compressor inlet is about 6 bar. So the compensate calculation is also needed in this side. The next figure is based on compensate of both gas cooler inlet side and compressor inlet side. It shows the two systems' COP are all increased and are close to each other on the same gas cooler outlet temperature. The discrepancy of two systems' performance can be neglected.

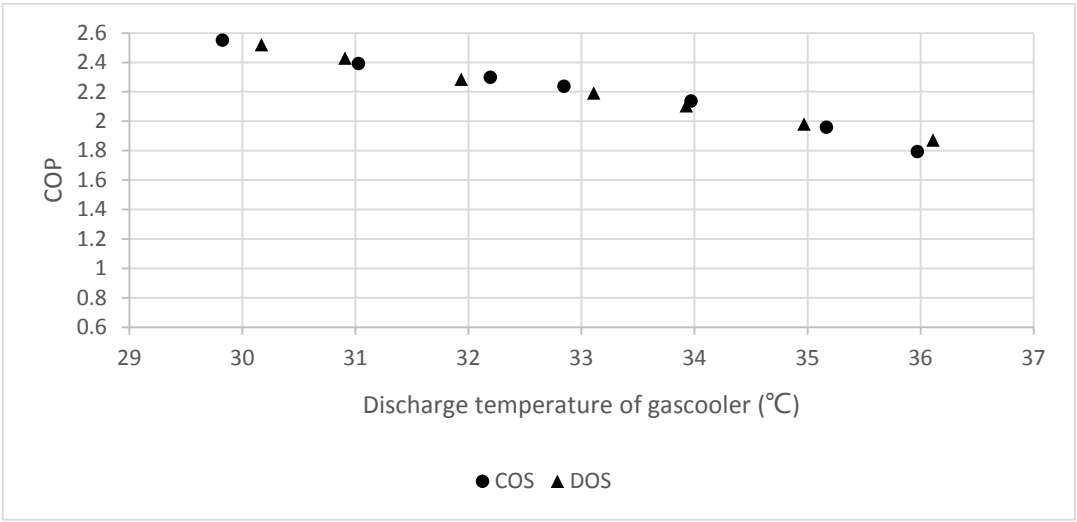

Figure 38 Compensated COP from both side

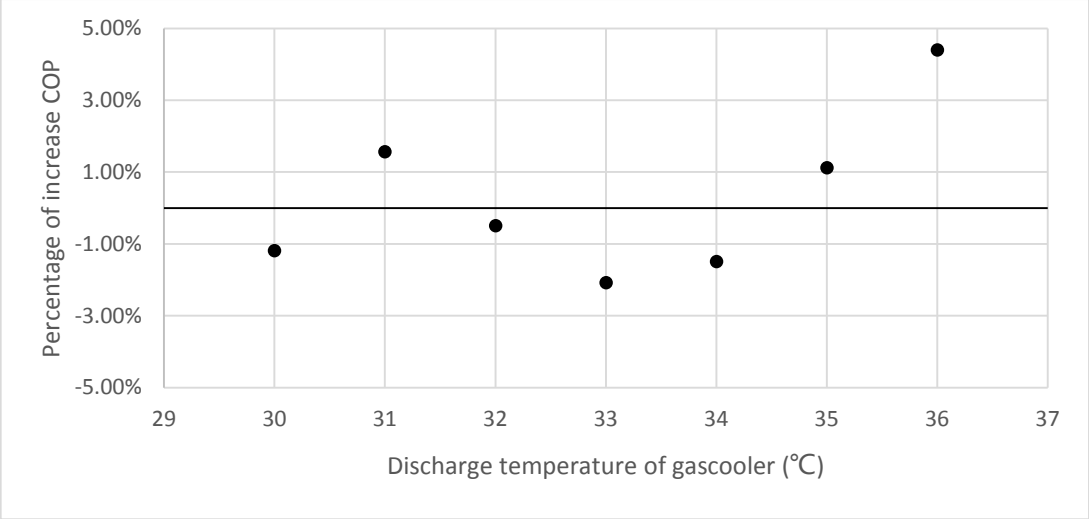

Figure 39 The percentage of increase (compensated COP of both side)

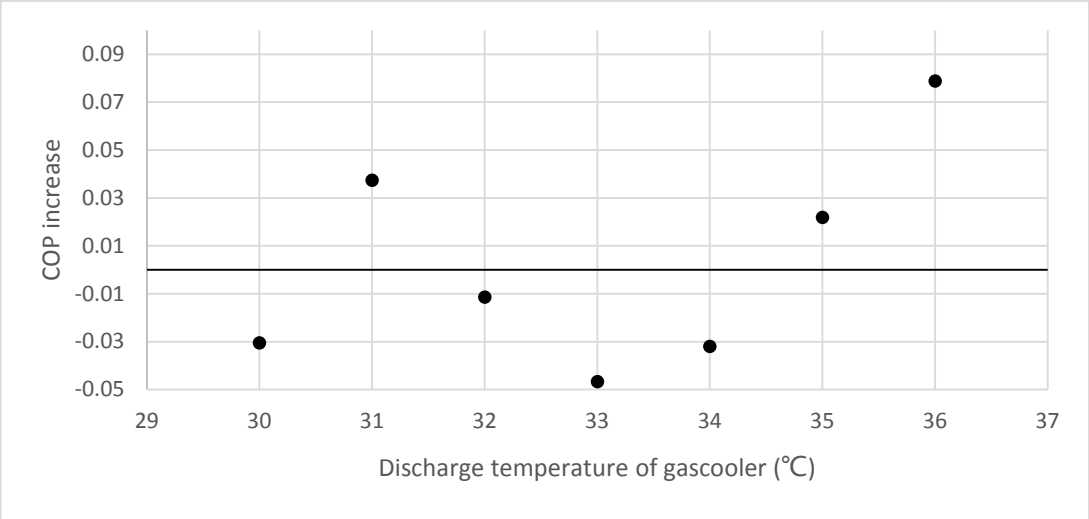

Figure 40 The increased COP (compensated from both side)

The exergy calculation is based on two evaporator. The specific exergy of a thermodynamic state is defined in equation from Moran and Shapiro(2008). The specific exergy due to the kinetic and potential energy has been neglected. The exergy has be defined in reference to the thermodynamic dead state which has been defined as glycol and water at 294.15 K and 101 kPa for the analysis. The exergy efficiency is defined as the increased exergy of air evaporator and glycol evaporator divides by compressor work.

$$\varphi = h - h_0 - T_0(s - s_0) \tag{5-4}$$

$$\eta_{exergy} = \frac{(\varphi_{out} - \varphi_{in})_{glycol} + (\varphi_{out} - \varphi_{in})_{air}}{W_{comp}} \tag{5-5}$$

In the exergy analysis, it shows the same pattern as the COP analysis before. At the beginning the DOS system is better than the COS system. With the compensation from compressor discharge side, the difference between two systems becomes smaller. When compensate from compressor inlet and discharge side, the difference between two systems becomes even smaller. In this analysis, the DOS is more tolerant to the poor system design, it can work better than the COS system when the pressure drop cannot neglect on the pipe line.

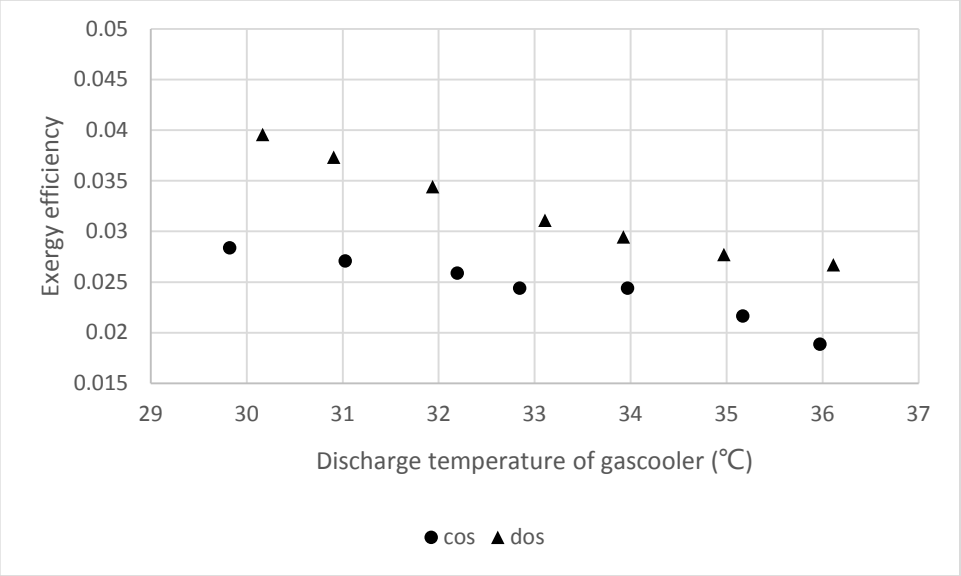

Figure 41 Exergy efficiency

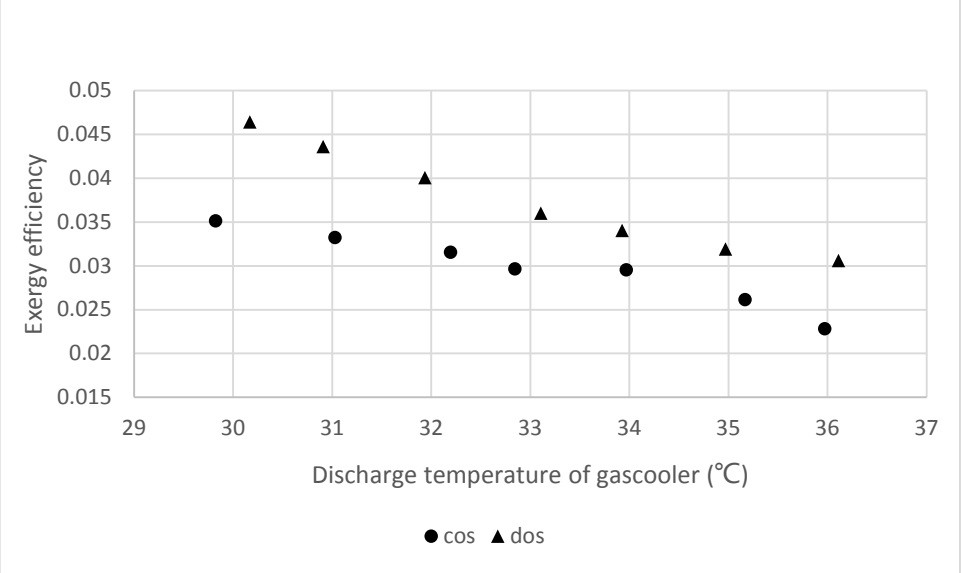

Figure 42 Compensate exergy efficiency from Compressor discharge side

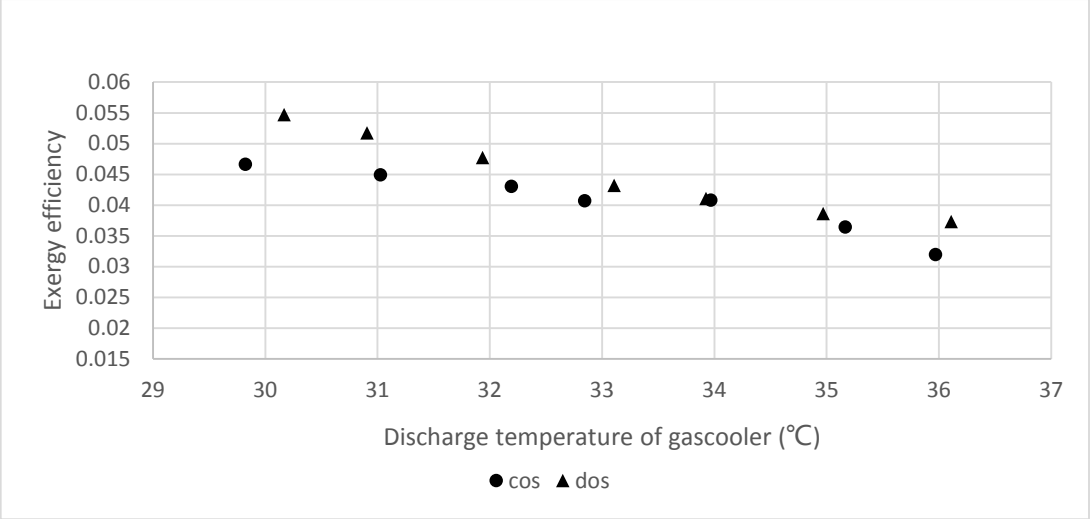

Figure 43 Compensate exergy efficiency from both side

5.3 Uncertainty analysis

There are always differences between the measurement and the real value. So it is important to analysis the uncertainty in research process. The obtained results might be considered complete when they are attached of the extract of its uncertainty. The method in order to determine the process uncertainty was selected from the Guidelines for Evaluating and Expressing the Uncertainty of NIST Measurement Results (1994). There are two different categories in the experimental uncertainty:

Type A: The uncertainty evaluation of a series of observations by the statistical analysis.

Type B: The uncertainty evaluation of a series of observations by means other than the statistical methods.

The type A uncertainty is based on any statistical method for treating data, such as taking the standard deviation of a series of independent observations. However, the type B uncertainty B is based on scientific judgement by means of all relevant information available to the operator, like using calibration reports or manufacturers references.

On the one hand, the type A error denoted is defined as the standard deviation of the obtained measurements in the phase of six minutes in a specific test point condition. The sample is determined as:

$$x_i = \overline{X}_i = \frac{1}{n}\sum_{k=1}^{n} X_{i,k} \tag{5-5}$$

Then the standard deviation of type A is:

$$u_A = s(\overline{X}_i) = (\frac{1}{n(n-1)}\sum_{k=1}^{n}(X_{i,k} - \overline{X}_i)^2)^{1/2} \tag{5-6}$$

On the other hand, the uncertainty type B is calculated by the sensor accuracy from its manufacturer's references. The sensor accuracy is used to establish upper $a_+$and lower a_- limits for the obtained measurements. The probability that all values obtained are in the determined range is assumed to be 100%. The probability is calculated by a rectangular distribution, so it is equally probable that the obtained values will be inside the limited range. Then, being the uncertainty calculated as:

$$u_B = \frac{a}{\sqrt{3}} \tag{5-7}$$

Where,

$$a = \frac{(a_+ - a_-)}{2} \tag{5-8}$$

The combined uncertainty is calculated as a function of the measured values by the law of propagation of uncertainties with uncertainty components estimated as standard deviations.

The combined uncertainty is calculated by:

$$u_c = \sqrt{(\frac{\partial f}{\partial x})^2 u_i^2(x) + (\frac{\partial f}{\partial y})^2 u_i^2(y)} \tag{5-9}$$

Where the partial derivatives is calculated by:

$$\frac{\partial f}{\partial x} = \frac{f(x + dx, y) - f(x, y)}{dx} \tag{5-10}$$

Thus, the combined uncertainty could be either the type A or type B can be related with the quantity x or y, which results in the combined uncertainty A and B, respectively. In the last equation, the covariance between the uncertainty of x and y is assumed to be zero.

Some sample values of uncertainty for measured parameters are presented in next two table.

Table 10 Combined uncertainty of first experiment

Parameter	Unit	Combined uncertainty

Evaporating temperature	℃	±(0.15)
Motive nozzle temperature	℃	±(0.25)
Gas cooler outlet pressure	MPa	±(0.013)
Ejector outlet pressure	MPa	±(0.006)
Motive nozzle mass flow	kg/min	±(0.004)
Suction nozzle mass flow	kg/min	±(0.004)
Ejector efficiency	-	±(0.002)

Table 11 Combined uncertainty of second experiment

Parameter	Unit	Combined uncertainty
Motive nozzle pressure	MPa	±(0.006)
Motive nozzle temperature	℃	±(0.13)
Suction nozzle pressure	MPa	±(0.006)
Suction nozzle temperature	℃	±(0.25)
Motive nozzle mass flow	kg/min	±(0.006)
Suction nozzle mass flow	kg/min	±(0.005)

5.4 Summary of this chapter

This chapter shows the experimental analysis of two experiment. First one is overall view of ejector performance, it shows where the high efficiencies lies on the working conditions. The results can guide the test points choosing on the second experiment. Second one is comparison of two systems, which are Burk cycle (DOS) and Oshitina cycle (COS). The comparisons are about the two systems' COP and exergy increase in the evaporator side. Then the uncertainty analysis is introduced to complete the experimental analysis.

6. Computational simulation

This part describes a model developed based on Kornhauser ejector model. This model requires the motive inlet pressure, motive inlet specific enthalpy, the suction inlet pressure and specific enthalpy, the mass flow of both the motive side and suction side as the model inputs. These values have already measured during the experimental investigate before. This model also need to assume the isentropic efficiencies of the motive nozzle, the suction nozzle and the diffuser. The assumptions and the applied equations in the thermodynamic model are described below. The comparisons of the model results and experimental results are also presented below.

6.1 Thermodynamic ejector model

The model is developed to predict and improve the efficiency of ejector and pressure lift on different condition. For all the ejector parts, the model use 1D models. Rapid parameters changes and shock waves due to the high velocity difference between the motive stream and suction stream make the use of a more realistic model very difficult. Therefore the 1D model is developed based on the Kornhauser model [17]. There are four main parts of the ejector: the motive nozzle, the suction nozzle, the mixing section and the diffuser. Description of the program general principles and detailed descriptions of the various parts together with the equations applied in the model are presented.

The program called Engineering Equation Solver (EES) [18] is used to build the ejector model. EES is a powerful mathematical program similar to Matlab. It can also solve very difficult mathematic problem, which in this case are the equations that describe the different parts of ejector. But the difference between EES and Matlab, the former contains the thermophycical properties of many common substances used in thermal science application, makes EES more suitable to build the ejector model.

Most of the simulations described the ejector models in an essentially one-dimensional fashion. The most important part is the mixing process. There are three ways used to describe this process: with the mixing at constant pressure, with the mixing at constant area, and with a combination of constant pressure and constant area mixing. In this model constant pressure mixing was assumed. And other assumptions and equations that describe the ejector parts are present below.

The model assumes that:

1. There is no pressure drop in all the heat exchangers and the pipe lines. And there is no kinetic energy outside the ejector.
2. There is no heat transfer from or to the environment except the gas cooler and the evaporator.
3. The compressor works in a certain specified isentropic efficiency.
4. The heat exchanger transfer the heat at no temperature difference. That is to say in the heat transfer th e LMTD is 0 K.
5. In the ejector mixing section the two streams mix at a constant pressure.
6. Except the mixing section the properties and velocities of refrigerant are constant, which is to say the model is one dimensional.
7. The refrigerant is at all time in thermodynamic equilibrium. With the assumption 6, it is known in two-phase flow as homogenous equilibrium model.
8. Refrigerant leaves the evaporator is saturated liquid.

When it comes to calculation, there are four parts of the ejector. Use the DOS cycle as the example, the COS will be the same.

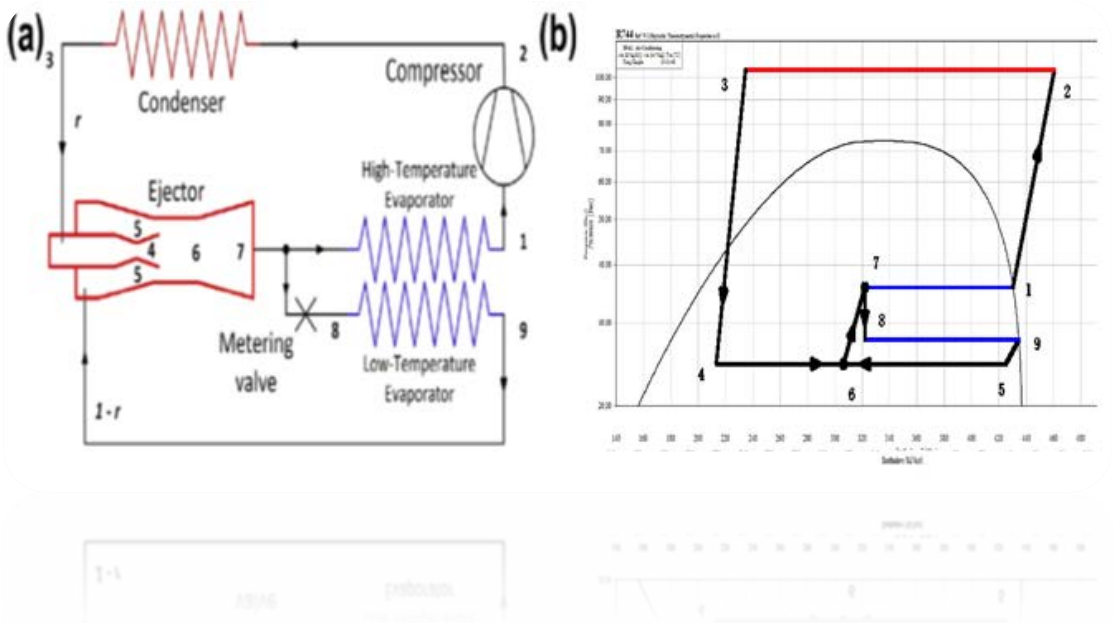

Figure 44 The representation of DOS cycle

The motive nozzle:

The motive nozzle isentropic efficiency is defined as the real specific enthalpy divides by the isentropic specific enthalpy increase. And with all the assumption above, the increased specific enthalpy can be the increased kinetic energy.

$$\eta_{mn} = \frac{h_3 - h_4}{h_3 - h_{4,isen}} \tag{6-1}$$

$$\frac{1}{2}V_4^2 = h_3 - h_4 \tag{6-2}$$

V_4 is the velocity of the point 4 showed in fig.

η_{mn} is the isentropic efficiency of the motive nozzle.

The suction nozzle:

The suction nozzle isentropic efficiency is defined as the real specific enthalpy divides by the isentropic specific enthalpy increase. And with all the assumption above, the increased specific enthalpy can be the increased kinetic energy.

$$\eta_{sn} = \frac{h_9 - h_5}{h_9 - h_{5,isen}} \tag{6-3}$$

$$\frac{1}{2}V_5^2 = h_9 - h_5 \tag{6-4}$$

V_5 is the velocity of the point 5 showed in fig.

η_{sn} is the isentropic efficiency of the suction nozzle.

The mixing section:

The mixing section is the most important parts of the ejector. With the assumption above, the two streams are mixing on the constant pressure. The specific enthalpy and the velocity can calculated below.

$$h_6 = \phi h_4 + (1 - \phi)h_5 \tag{6-5}$$

$$V_6 = \phi V_4 + (1 - \phi)V_5 \tag{6-6}$$

ϕ is the mass flow ratio of the motive nozzle and the suction nozzle.

The diffuser isentropic efficiency is defined as the real specific enthalpy increase divides by the kinetic energy loss in this process which is equal to the isentropic enthalpy increase.

$$\eta_{diff} = \frac{h_7 - h_6}{\frac{1}{2}V_6^2} \tag{6-7}$$

$$\frac{1}{2}V_6^2 = h_{7,isen} - h_6 \tag{6-8}$$

η_{diff} is the diffuser isentropic efficiency.

So the inputs of this model are the pressure and specific enthalpy of the motive nozzle and suction nozzle inlet, the mass flow ratio, three isentropic efficiencies above and the mixing pressure. Outputs are the pressure P_7 and specific enthalpy T_7 of the diffuser.

6.2 Comparison between ejector model results and experimental results

Initially, the calculation results are not acceptable, mainly because the assumption of the three efficiencies is too high. In the assumptions above, the friction and disequilibrium is neglected. These factor will also influence the three efficiencies. When the three efficiencies set to lower values, the calculation results are more accurate compare to the real results.

In the first experiment, the focus is on the overall performance of the ejector. Using the measurement as the inputs of the ejector model, which has discussed above. The mixing pressure is assumed as the pressure of the refrigerant at the temperature $(T_9 - 0.5)$ ℃ and the specific entropy s_9. With the inputs from the measurement and the assumptions above. Some of the outputs comparison between the model and the experiment is in the next table.

Table 12 comparison between the model and the experiment

Experi-mental P_7/bar	Calculated P_7/bar	Difference	Experi-mental T_7/K	Calculated T_7/K	Difference
30.26	30.07	-0.19	268.5	267.7	-0.9
31.77	31.67	-0.10	270.3	269.6	-0.7
32.21	32.01	-0.20	270.8	270.0	-0.9
30.36	30.16	-0.20	268.7	267.8	-0.9
31.29	30.87	-0.42	269.8	268.6	-1.1
32.24	31.52	-0.72	270.9	269.4	-1.5
33.16	32.66	-0.50	271.9	270.7	-1.2

All the test points in the first experiment have been used as the inputs in the ejector model. The discrepancy between the experimental results and the calculated results are showed in the fig below. The X axis is the measured diffuser outlet pressure in bar and the measured diffuser outlet temperature in K. The Y axis is the calculated diffuser outlet pressure in bar and the calculated diffuser outlet temperature in K. The discrepancy between the pressures is about 5%, which means the ejector model can very well predict the ejector performance on the pressure side. The discrepancy between the temperatures is below 1%, but it is not to say the ejector model can predict the ejector performance on temperature side more accurate. Because the comparison between temperature uses K as the unit. The reason using K as the unit is the temperature of the diffuser outlet is close to 0 ℃. When using the ℃ as the unit, the discrepancy will not affect the difference between temperature correctly. So the biggest difference between temperatures between measured and calculated is needed to describe the ejector model's ability to prediction. The biggest difference between temperatures is about 2 K. That seems to be a very big difference, but considering the diffuser outlet properties is far away from the critical point of R744, the difference between temperatures doesn't affect the enthalpy of R744 very much. In conclusion, the ejector model can well predict the ejector performance in the working condition as the experiment taking. So the ejector model can utilize in the system simulation, in this case, the Condenser outlet spilt cycle and the Diffuser outlet spilt cycle. The system simulation setup and comparison will be discussed in the next chapter.

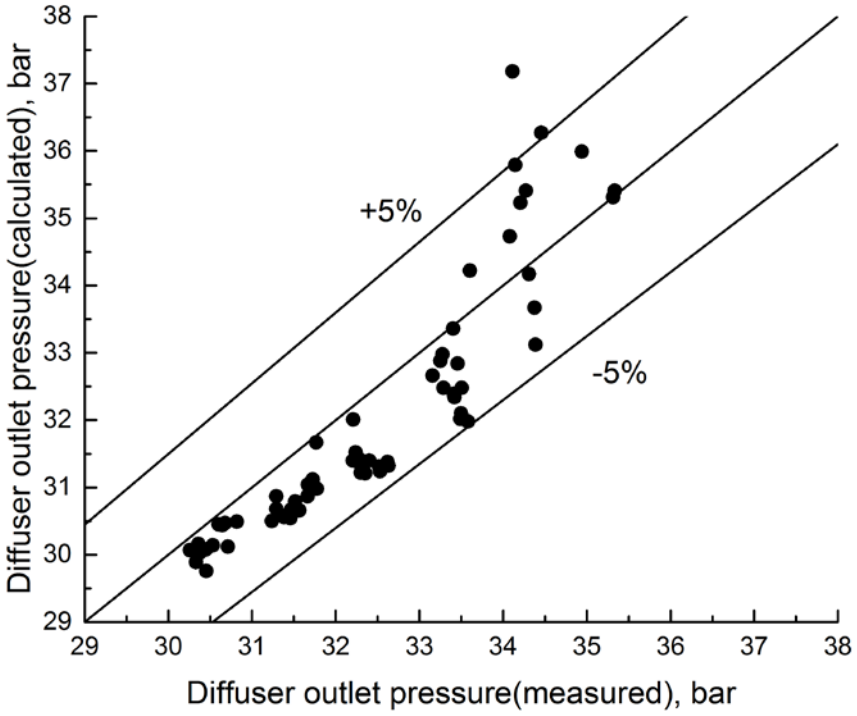

Figure 45 The difference between diffuser outlet pressures (measured and calculated)

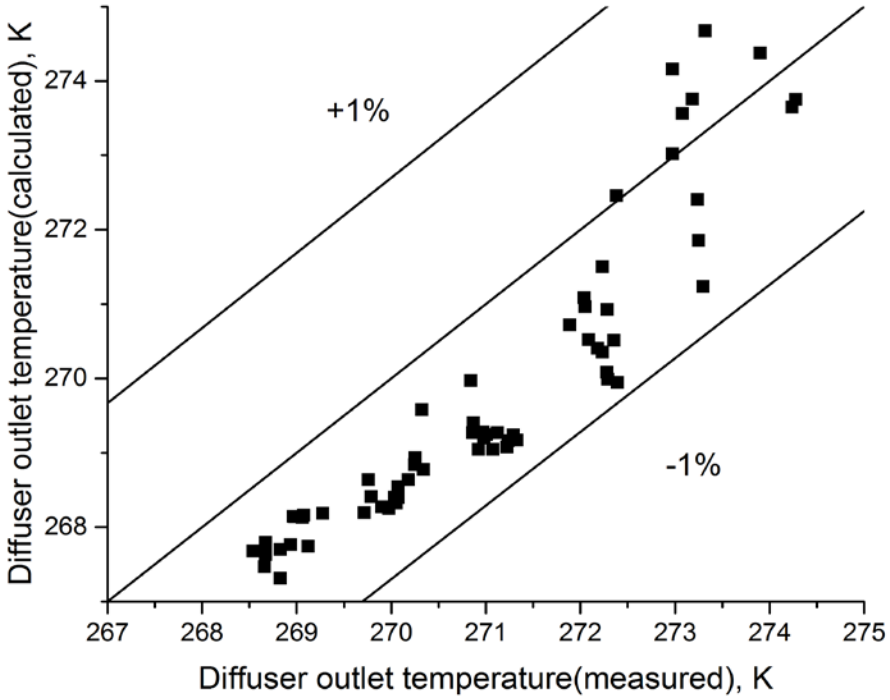

Figure 46 The difference between diffuser outlet temperatures (measured and calculated)

There is another side to see whether the model can reflect the real process in the ejector chamber. The pressure difference between the motive nozzle inlet and the diffuser outlet $\Delta P_{mn-diff}$ and the pressure difference between the diffuser outlet and the suction nozzle inlet $\Delta P_{diff-sn}$. Some of the test points and calculated points are in the next table.

Table 13 Test points and calculated points

$\Delta P_{mn-diff}$/bar (experimental)	$\Delta P_{mn-diff}$/bar (calculated)	Difference/bar	$\Delta P_{diff-sn}$/bar (experimental)	$\Delta P_{diff-sn}$/bar (calculated)	Difference/bar
30.86	2.34	0.19	2.34	2.15	-0.19
28.42	2.34	0.10	2.34	2.24	-0.10
27.43	2.52	0.20	2.52	2.32	-0.20
31.70	2.22	0.20	2.22	2.02	-0.20
30.23	2.69	0.42	5.08	5.73	0.65
29.27	3.58	0.72	5.00	4.96	0.04
28.67	4.48	0.50	4.48	3.98	-0.50

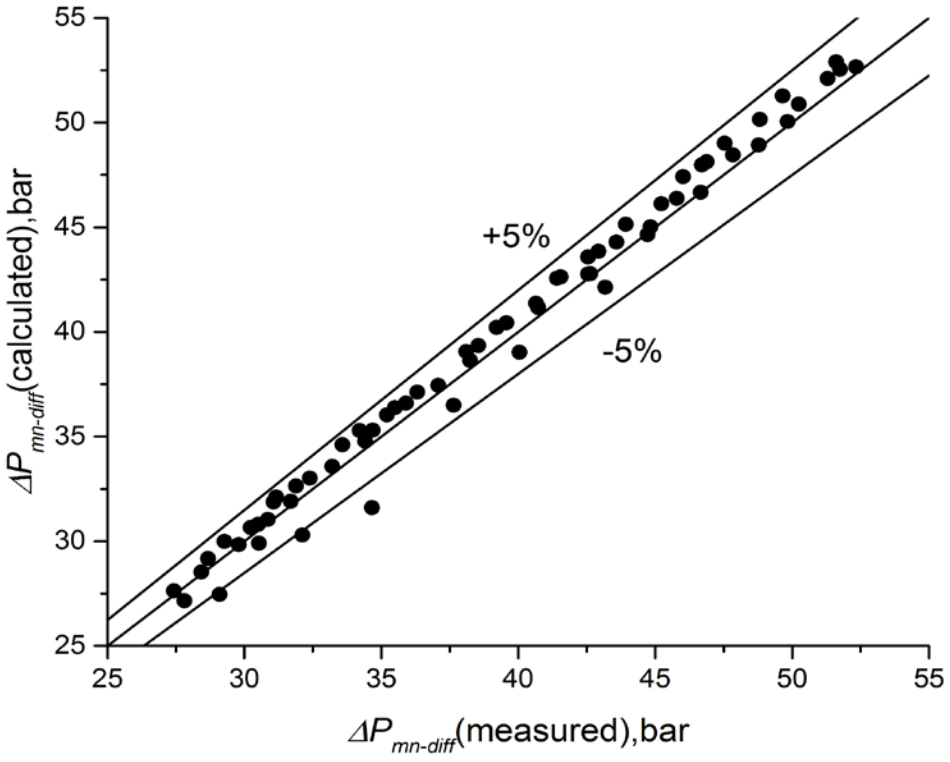

Figure 47 The difference between $\Delta P_{mn-diff}$ (measured and calculated)

The comparison of the pressure differences between measured and calculated of some test points are presented in the fig above.

The fig above shows that the pressure difference between the motive nozzle inlet and the diffuser outlet. In the X axis is the measured pressure difference and the Y axis is the calculated pressure difference. The difference between the two pressure differences is less than 5%, which should be a very well prediction.

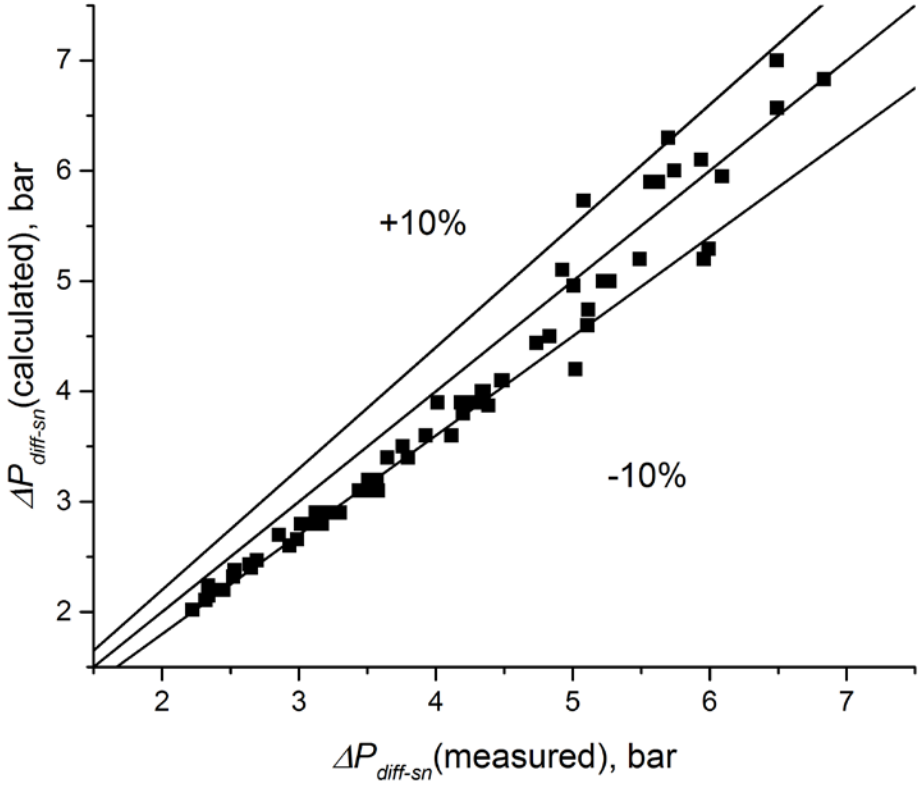

Figure 48 The difference between $\Delta P_{diff-sn}$ (measured and calculated)

The fig above shows that the pressure difference between the diffuser outlet and the suction nozzle inlet. In the X axis is the measured pressure difference and the Y axis is the calculated pressure difference. The difference between the two pressure differences is less than 10%, which is not a very well prediction. Because the pressure difference in this case is not that big, it is less than 10 bar. So the difference between the measurement and calculation maybe as small as the difference in the above case, but the percentage will be bigger than the above case. There are also some limitations of this ejector model that may cause the difference between measurement and calculation. The limitations of this analysis will be discussed on the last of this chapter.

6.3 Comparison between the COS cycle and DOS cycle

The second objective of the thesis is to compare the performances of COS and DOS cycles. The experimental methods are discussed in the above chapter. This part will discuss the computational methods and use them to compare these two cycles.

The setup of the two cycles are basis on the ejector model built above. The gas cooler, the high temperature evaporator and the low temperature evaporator are working on constant pressure. And there are no pressure drop on the pipe lines. Because the pipe line pressure drop is too big to neglect in experiment. So in the simulation, the ejector inlet pressure will be use as the gas cooler outlet pressure. The compressor is working on an isentropic efficiency as in the experiment. The total refrigeration load is also given the same as in the experiment. The comparison of the COP between the experimental measured and the simulation are listed on the next table.

Table 14 comparison of the COP between the experimental measured and the simulation

COS			DOS		
Gas cooler outlet temperature, ℃	COP（measured）	COP（calculated）	Gas cooler outlet temperature, ℃	COP（measured）	COP（calculated）
30	1.16	1.24	30	1.55	1.34
31	1.05	1.12	31	1.47	1.48
32	0.98	0.98	32	1.37	1.49
33	0.94	1.00	33	1.29	1.35
34	0.88	0.95	34	1.23	1.28
35	0.76	0.85	35	1.14	1.25
36	0.65	0.71	36	1.05	1.17

In the next fig, it shows the discrepancy between the COP based on measurement and the COP based on calculation. The difference of COS cycle and DOS cycle are about 10%. The simulation can well reflect the experiment condition. These two cycles are not well designed in the test rig. The pipe line pressure drop makes the cycles working as a lower gas cooler pressure system. When the system working as transcritical, if the working pressure of

the gas cooler is close to the critical point of R744, the COP of the system will drop dramatically. With the simulation of the two cycle, it can also explain the low COP of two system.

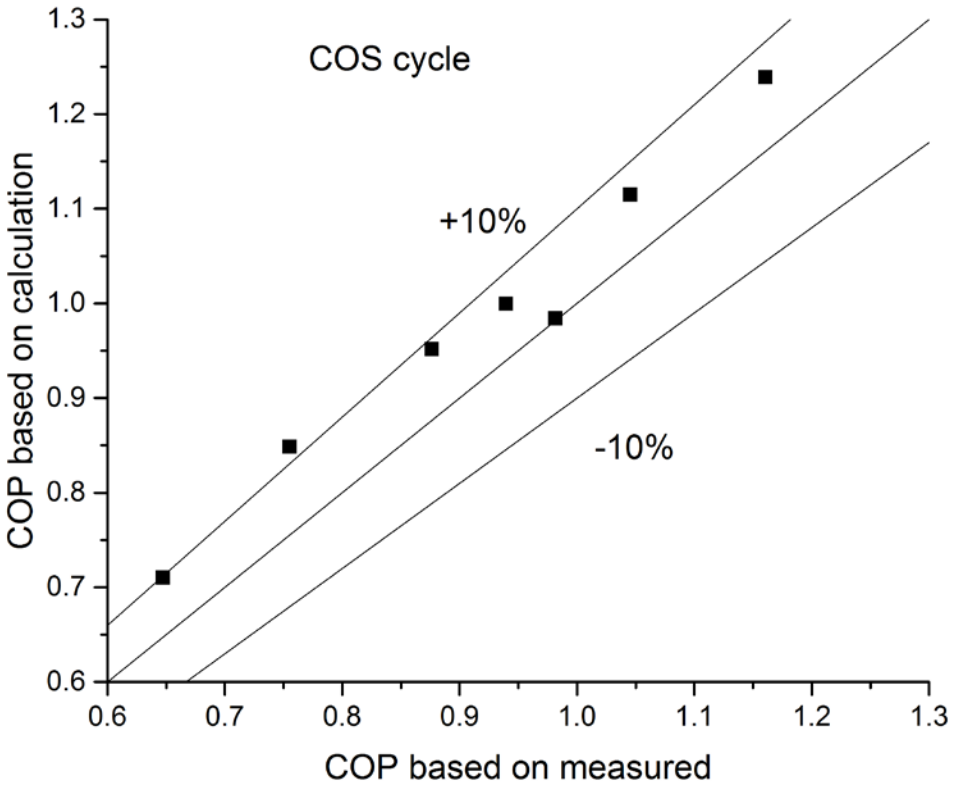

Figure 49 The discrepancy between COS cycle's COP

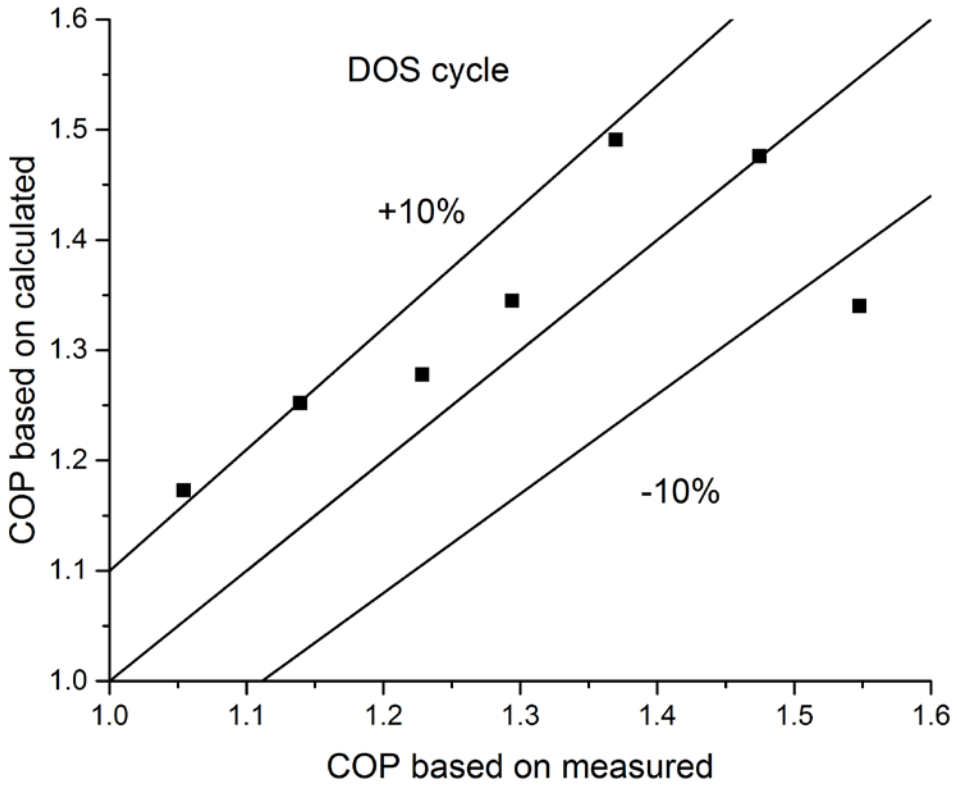

Figure 50 The discrepancy between DOS cycle's COP

6.4 Comparison between the two cycles and simulated expansion valve cycle

In order to know the COS and DOS system is better than the normal expansion valve cycle, the comparison between the two cycles and expansion valve cycle should be done. Due to the limitation of the test rig, it cannot realize three cycles simultaneously, the expansion valve cycle performance is investigated by numerical method. The demonstration of expansion valve cycle is in next figure.

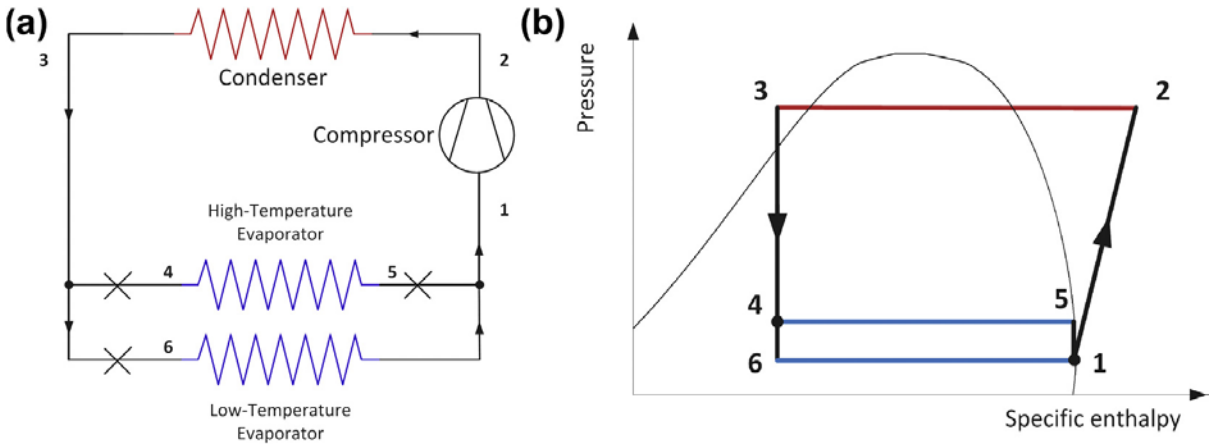

Figure 51 Expansion valve cycle layout and pressure-specific enthalpy diagram (Lawrence 2013)

In order to compare these cycles evenly. Some assumption have been made on the expansion valve cycle. The working pressure of gas cooler is the same as the COS and DOS system. The mass flow rate of R744 is the same. The load and temperature of two evaporator is the same. The mass flow rate of high-temperature evaporator which is the glycol evaporator and low-temperature evaporator which is the air evaporator is also the same. In a word, the gas cooler and the two evaporator is working in the same condition between the experiment and simulation. The COP of three cycles are shown in next table.

Table 15 The COP of three cycles

Gas cooler outlet temperature, ℃	COS cycle	DOS cycle	Expansion valve cycle
30	1.16	1.55	0.92
31	1.05	1.47	0.89
32	0.98	1.37	0.87
33	0.94	1.29	0.86
34	0.88	1.23	0.83
35	0.76	1.14	0.74
36	0.65	1.05	0.63

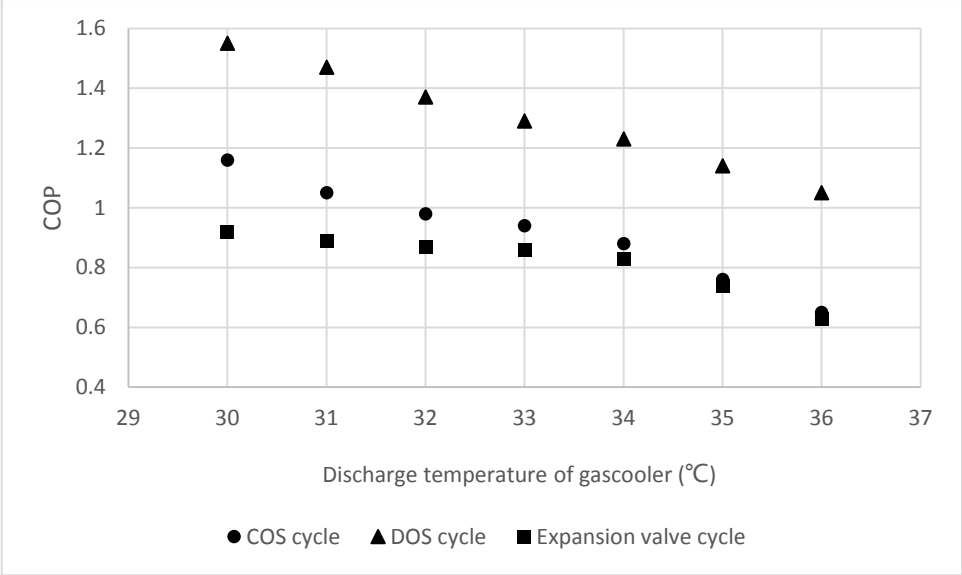

Figure 52 The COP of three cycles

The results show that in every test point, the COP of the COS and DOS cycles are higher than expansion valve cycle in 23% and 48% respectively. That means such systems with ejector can never perform poorly than a normal expansion valve cycle. Because with the no entrainment flow, the ejector is working just like an expansion valve. With the comparison with the expansion valve cycle, it can see clearly how the ejector increases the system performance. The test rig is not optimized, so the COP of two tested cycle are not high. But through the comparison with the normal expansion valve cycle, it can see that the ejector truly increases the system performance. Due to the losses are too huge in the whole system, the COP of these two systems are relatively low.

6.5 Optimize the two cycles through numerical methods

As talked before, the system is not optimized. There are big pressure losses in the pipe line. So in this part, these two cycles will be simulated in the condition that there are no pressure losses. The results compared to the experimental results are shown in next table

Table 16 The comparison of experimental COP and ideal simulation COP

Gas cooler outlet temperature, ℃	COS cycle		DOS cycle	
	Experimental COP	Ideal simulation COP	Experimental COP	Ideal simulation COP
30	1.16	2.76	1.55	2.93

31	1.05	2.66	1.47	2.84
32	0.98	2.54	1.37	2.73
33	0.94	2.46	1.29	2.59
34	0.88	2.33	1.23	2.51
35	0.76	2.03	1.14	2.41
36	0.65	1.82	1.05	2.32

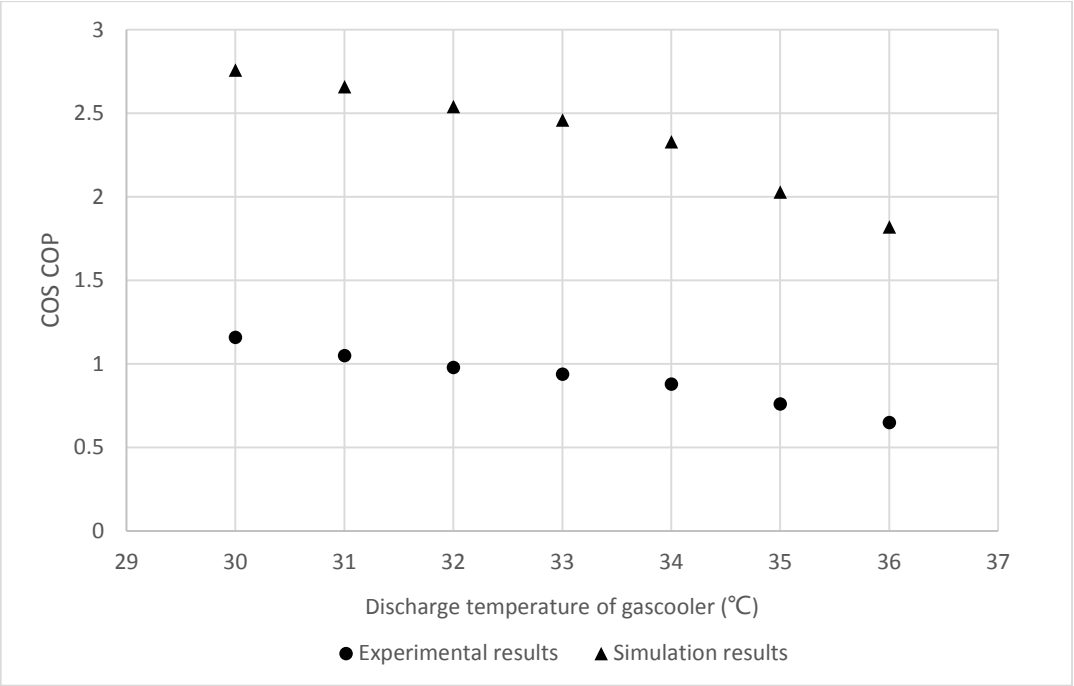

Figure 53 The comparison of COS COP

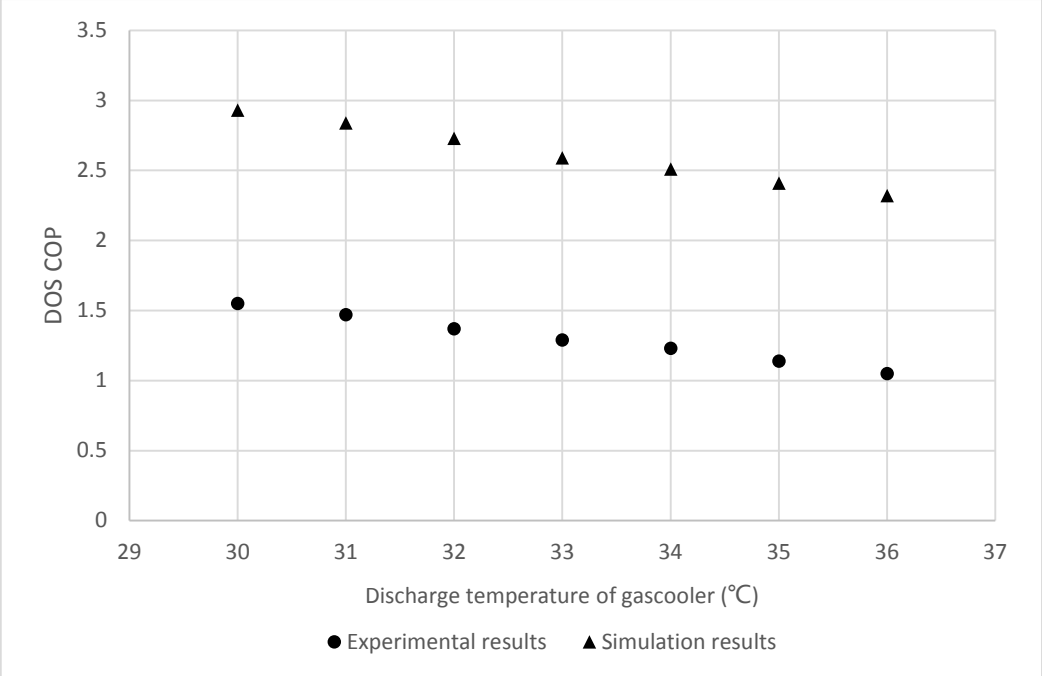

Figure 54 The comparison of DOS COP

The results show that the ideal simulation which with no pressure losses through pipe line has a much better COP than the real experiment. With the comparison between the COP, it shows that the pressure losses in the compressor inlet and discharge side are the main reason that cause the low COP in the two cycles. When it comes to design the ejector system, the pressure losses should be considered. And the pipe should be chosen to fit the mass flow of the refrigerant. But when compare the two simulated COP of COS and DOS system, it can be found that the DOS system is slightly better than COS system. The reason is the system pressure is controlled automatically by the temperature setting. So even the two system running at the same gas cooler outlet temperature, the compressor outlet pressure is different. The DOS system running in a lower gas cooler pressure than COS system when the gas cooler outlet temperature is the same. That is because the pressure losses cannot be exactly same in the two system. The DOS system has lower pressure losses. So the compressor work is also small in the DOS system. That is the reason, even the theoretical COP of the two system is same, the DOS system works better than COS system.

6.6 Limitations of model

The one-dimensionality of this model is intrinsically limiting. The details of flow patterns and temperature gradients within the ejector cannot be considered within its framework. It would be better to increase the sophistication of the one-dimensional model by replacing nozzle and diffuser efficiencies with friction factors and shock calculations, which have done by Krzysztof. Considering the complexity of the model, the simpler model is chosen here.

The assumption of cross-sectional homogeneity and thermodynamic equilibrium is clearly incorrect. Numerous studies have shown that a saturated liquid expanding through a nozzle is in a non-equilibrium inhomogeneous state, it appears that the flow typically consists of a core of metastable liquid surrounded by an annulus of saturated vapor. The non-equilibrium condition of the fluid leaving the nozzle may have important implications tor ejector performance.

The assumption of constant pressure mixing is not particularly limiting. Some performance improvements might be obtained by using constant area mixing or a combination of constant pressure and constant area mixing (Keenan et al, 1950), but they would not be dramatic.

This model does not address the problem of off-design performance. In general, ejectors perform poorly away from their design points, so this limitation may be important.

6.7 Summary of this chapter

This chapter shows the computational simulation on the ejector and cycles. The ejector model is developed based on Kornhauser ejector model. The assumptions and the applied equations in the thermodynamic model are described below. The comparisons of the cycle model results and experimental results are also presented below. At last an expansion valve cycle is built to present how the ejector can help improving the system performance. Some limitation of the model are shown.

7. Conclusion

This paper begins with the development of ejector, then the theory of ejector working principle and the description of the cycles that mainly focused on this paper are presented. Below that is two experimental analysis: first one focus on the overall efficiency of the ejector used in the experiment and second one the comparison between two kinds of cycle that talked before in the theory part. Some simulation works are done to support the experimental results.

In the first experiment, the result obtained show that the ejector works more efficiently when the pressure ratio is from 1.11 to 1.18 and the entrainment is from 0.4 to 0.7 approximately. The highest efficiency is 0.389, it was achieved by the discharge pressure is 6.5 MPa, the motive inlet temperature is 23.2 degree centigrade, the entrainment ratio is 0.56, the pressure is 1.132 and the pressure lift is 0.376 MPa approximately. It can also see from the result that he high efficiency can be achieved in the medium pressure ratio with respective discharge pressure, and with the motive inlet temperature raising the higher efficiency show up in higher pressure. These experimental results can be a guide to the following experiment. With the knowledge of the performance of ejector at different working condition, it is easy to choose a working condition for building the system and making the experiment plan.

In the second experiment, the result shows that the DOS system works well than COS system, mainly because the discharge pressure of the compressor is lower of DOS system at the same gas cooler discharge temperature and the same refrigeration load. Due to the lower discharge pressure of the compressor the compressor load is less and the gas cooler load is also less. In the two system, the refrigeration load is the same, so the compressor work represents the system's COP. The DOS system's compressor work is less than COS, so the COP of DOS system is higher than the COS system. But with the compensate calculation of the compressor discharge and inset, the two systems' COP are almost the same, which is fit the theoretical situation from Lawrence and Elbel(2013). In the experiment, the result also shows that, when the system is not optimized the DOS system are more suitable than COS system with the pressure drop in the pipe line.

At last, simulation works are done to support the experimental results. In the ejector simulation, the discrepancy between the pressures is about 5%, which means the ejector model can very well predict the ejector performance on the pressure side. The discrepancy between

the temperatures is reasonable. So the ejector model can well predict the ejector performance in the working condition as the experiment taking. In the system simulation, the discrepancy between the COP based on measurement and the COP based on calculation is reasonable. The difference of COS cycle and DOS cycle are about 10%. The simulation can well reflect the experiment condition. Then the experimental results are compare to a simulated expansion valve cycle, in order to see how the ejector helped the system performance. Below that part, some limitations of experiment are optimized by the numerical methods. The results show that the pressure losses are the main reason that cause the low COP in both system. Some limitations of the simulation is also discussed.

8. References

[1] Elbel, Stefan. "Historical and present developments of ejector refrigeration systems with emphasis on transcritical carbon dioxide air-conditioning applications." International Journal of Refrigeration 34.7 (2011): 1545-1561.

[2] Gay, N.H. 1931. Refrigerating system. U.S. Patent No. 1836318.

[3] Lawrence, Neal, and Stefan Elbel. "Theoretical and practical comparison of two-phase ejector refrigeration cycles including First and Second Law analysis." International Journal of Refrigeration 36.4 (2013): 1220-1232.

[4] Groll, Eckhard A. "Ejector technology." (2011): 1543-1544.

[5] Ozaki, Y., Takeuchi, H., Hirata, T., 2004. Regeneration of expansion energy by ejector in CO2 cycle. Proceedings of the 6th IIR-Gustav Lorentzen Conference on Natural Working Fluids, Glasgow, UK.

[6] Li, D., Groll, E.A., 2005. Transcritical CO2 refrigeration cycle with ejector-expansion device. Int. J. Refrigeration 28, 766e773.

[7] Henry, R.E., Fauske, H.K., 1971. Two phase critical flow of one component mixtures in nozzles, orifices, and short tubes. J. Heat Transfer 93, 179e187.

[8] Elbel, S.W., Hrnjak, P.S., 2004a. Effect of internal heat exchanger on performance of transcritical CO2 systems with ejector. 10th International Refrigeration and Air Conditioning Conference at Purdue, Paper R166, West Lafayette, IN, USA.

[9] Bergander, M.J., 2005. New Regenerative Cycle for Vapor Compression Refrigeration. Final Scientific Report, DOE Award DE-FG36-04GO14327. Madison, CT, USA.

[10] Liu, Fang, and Eckhard A. Groll. "Study of ejector efficiencies in refrigeration cycles." Applied Thermal Engineering 52.2 (2013): 360-370.

[11] Banasiak, Krzysztof, et al. "A CFD-based investigation of the energy performance of two-phase R744 ejectors to recover the expansion work in refrigeration systems: An irreversibility analysis." International Journal of Refrigeration 40 (2014): 328-337.

[12] Smolka, Jacek, et al. "A computational model of a transcritical R744 ejector based on a homogeneous real fluid approach." Applied Mathematical Modelling37.3 (2013): 1208-1224.

[13] Dokandari, Damoon Aghazadeh, Alireza Setayesh Hagh, and S. M. S. Mahmoudi. "Thermodynamic investigation and optimization of novel ejector-expansion CO2 and

NH3 cascade refrigeration cycles (novel CO2 and NH3 cycle)." International Journal of Refrigeration 46 (2014): 26-36.

[14] Xing, Meibo, Jianlin Yu, and Xiaoqin Liu. "Thermodynamic analysis on a two-stage transcritical CO2 heat pump cycle with double ejectors."Energy Conversion and Management 88 (2014): 677-683.

[15] Lucas, Christian, et al. "Numerical investigation of a two-phase CO2 ejector." International Journal of Refrigeration (2014).

[16] Minetto, Silvia, et al. "Performance assessment of an off-the-shelf R744 heat pump equipped with an ejector." Applied Thermal Engineering 59.1 (2013): 568-575.

[17] Kornhauser, A.A., 1990. The use of an ejector as a refrigerant expander. Proceedings of the 1990 USNC/IIR-Purdue Refrigeration Conference, West Lafayette, IN, USA.

[18] EES (Engineering Equation Solver), 2007. Academic Professional Version 7.934-3D. F-Chart Software. Middleton, WI, USA.

[19] Oshitani, H., Yamanaka, Y., Takeuchi, H., Kusano, K., Ikegami, M.,Takano, Y., Ishizaka, N., Sugiura, T., 2005. Vapor Compression Cycle Having Ejector. U.S. Patent Application Publication US 2005/0268644 A1.

[20] Burk, R., Du¨ rr, G., Feuerecker, G., Kohl, M., Manski, R., Strauß, T., 2006. Vorrichtung zur Luftkonditionerung fu¨ r ein Kraftfahrzeug. D.E. Patent 10 2005 021 396 A1.

[21] Kemper, C.A., Harper, G.F., Brown, G.A., 1966. Multiple-Phase Ejector Refrigerating System. U.S. 3,277,660

[22] Newton, A.B., 1972a. Capacity Control for Multiple-Phase Ejector Refrigerating Systems. U.S. 3,670,519.

[23] Newton, A.B., 1972b. Controls for Multiple-Phase Ejector Refrigerating Systems. U.S. 3,701,264.

[24] Lawrence, N., Elbel, S., 2012. Experimental and analytical investigation of automotive ejector air conditioning cycles using low-pressure refrigerants. In: Proceedings of Int. Air Conditioning and Refrigeration Conference at Purdue, West Lafayette, IN, USA, Paper 2118.

[25] Klein, S.A., 2012. Engineering Equation Solver Academic Profession V9.206. F-Chart Software.

[26] S. He, Y. Li, R.Z. Wang, Progress of mathematical modeling on ejectors, Renewable and Sustainable Energy Reviews 13 (2009) 1760e1780.

A. Selvaraju, A. Mani, Analysis of an ejector with environment friendly refrigerants, Applied Thermal Engineering 24 (2004) 827e838.

[27] K. Smierciew, D. Butrymowicz, J. Karwacki, M. Trela, Modelling of ejection cycle for solar air-conditioning, international seminar on ejector/jet pump technology and application, 7e9 September 2009, Louvain-la-Neuve, Belgium, Paper No. 25.

[28] N.I. Kolev, Drag, lift and virtual mass forces. in: N.I. Kolev (Ed.), Multiphase Flow Dynamics 2, Thermal and Mechanical Interactions, third ed. Springer, Berlin, 2007, pp. 31e82.

[29] K. Banasiak, A. Hafner, 1D Computational model of a two-phase R744 ejector for expansion work recovery, Int. J. Therm. Sci. 50 (2011) 2235–2247.

[30] M. Nakagawa, A.R. Marasigan, T. Matsukawa, A. Kurashina, Experimental investigation on the effect of mixing length on the performance of two-phase ejector for CO2 refrigeration cycle with and without heat exchanger, Int. J. Refrig. 34 (2011) 1604–1613.

[31] Y. Zhu, W. Cai, Ch. Wen, Y. Li, Numerical investigation of geometry parameters for design of high performance ejectors, Appl. Therm. Eng. 29 (2009) 898–905.

Acknowledgements

I would like to express my gratitude to all those who helped me during the writing of this thesis.

My deepest gratitude goes first and foremost to Professor Wu Jingyi and Professor Eikevik, my supervisor of SJTU and NTNU, for their constant encouragement and guidance. She has walked me through all the stages of the writing of this thesis. Without her consistent and illuminating instruction, this thesis could not have reached its present form.

I would like to express my heartfelt gratitude to Krzysztof, who guides me all the stages of experimental work. I am also greatly indebted to Jin Zhequan, who give me a lot of advices in life and study in Norway.